Role of Fine Solids in Solvent Recovery from Reconstituted Alberta Oil Sands Gangue

by

Lawrence Ikenna Ejike

A thesis submitted in partial fulfillment of the requirements for the degree of

Master of Science

in

Chemical Engineering

Department of Chemical and Materials Engineering
University of Alberta

Abstract

Non-aqueous solvent extraction of bitumen from oil sands has the potential to replace the existing hot-water extraction process. The benefit of non-aqueous extraction process includes high bitumen recovery, reduction of fresh water demand for extraction and the elimination of resulting tailing ponds associated with the use of water. Other advantages include a significant reduction in energy consumption as well as greenhouse gas emission that are associated with ozone depletion and global warming. In the non-aqueous extraction process, bitumen is recovered from the ore using an organic solvent, leaving behind a gangue (solid waste) that contains residual bitumen, solvent, and water initially present in the ore. Despite its numerous advantages, a major limitation to NAE process is in minimizing the loss of solvent to the gangue. Recovery of solvent from the gangue is important to the economics of the non-aqueous extraction process and for environmental impact. Solvent recovery from the gangue involves a drying process in which the volatile solvent is evaporated from the porous gangue matrix in the presence of the water.

Fine solids in oil sands are known to have a detrimental effect on water-based extraction. Their role in non-aqueous extraction process has not been fully investigated. In this study, we examine the effect of fine solids content on the recovery of solvent from the gangue. Results from the compositional analysis of extracted gangue revealed that the composition of the gangue varies with each extraction. This presented a challenge to studying the interaction of solvent with other gangue components. A proper analysis of the effect of gangue components on solvent recovery from the gangue required well-defined parameters and a systematic control of the gangue composition. As such, a protocol was developed to make synthetic sample (reconstituted gangue) whose drying behaviour (fluid transport mechanism) simulated that of the extracted gangue. The reconstituted gangue was important as samples whose composition could be controlled to enable analysis and a definitive assessment of the effect of the components on solvent recovery from the gangue. Thus, the reconstituted gangues served as perfect substitutes for the extracted gangue.

Rich-grade solids (10% fines) and Low-grade solids (~20% fines) were used to prepare reconstituted gangue containing (i) 12% cyclohexane and (ii) 12% cyclohexane and 3.7 %* water (solvent free basis). Drying experiments were conducted on the samples in a fume hood at ambient temperature and pressure. All the drying experiments for samples containing only cyclohexane displayed a two stage drying process, with a fast initial rate drying stage and second slower drying stage. The first stage corresponded to the stage 1 evaporation of the solvent, in which liquid films maintain capillary connectivity to the external surface. In the slower second stage, liquid films had receded below the surface, and mass transfer occurred by diffusion within the porous media. For samples containing water, a third stage dominated by water diffusion followed the solvent-dominated drying stage. A comparison of drying curves for samples with similar liquid composition revealed that solvent removal was slower in low-grade samples compared to rich-grade samples. The particle size distribution and wettability of gangue solids were analyzed, and it was found that fine solids are more hydrophilic than coarse solids for each gangue. The effect of particle size distribution and wettability of solids of solids on the drying of porous media was investigated. Further experiments were performed for reconstituted gangue containing (i) 12% cyclohexane and (ii) 12% cyclohexane and 3.7% water (solvent free basis) for 0%, 10%, and 20% fines solids in each gangue grade. Results indicated that wettability of the fine solids had a dominant role on the drying of the gangue. An increase in fine solids content corresponded to a reduction in the solvent recovery and thus, an increase in solvent retention.

Acknowledgement

Table of Contents

List of Figures

List of Tables

1 Introduction

1.1 Background

Since the discovery of oil sands in Alberta and the development of the first technology to extract the oil in 1920, oil sands have grown in prominence as a means of securing Canada's energy future [1]. Canada is one of the world's leading sources of non-conventional oil and has the third largest proven crude oil reserves (approximately 170 billion barrels) in the world, next to Saudi Arabia and Venezuela [2]. The majority of this crude reserve is located in the Athabasca region of Alberta. Alberta's oil sands are a mixture of sands, fine solids (predominantly clay), water and crude bitumen. Crude bitumen is a highly viscous crude oil characterized by high density, high metal concentration, and a low hydrogen-to-carbon ratio compared to conventional (light) crude oil [1].

Crude bitumen in oil sands is believed to have formed from the bacteria degradation of light crude oil trapped in rock pores in oil reservoir over millions of years. Bacterial attack depleted the oil of the light hydrogen rich fractions (alkanes), leaving behind the higher molecular weight fraction [3]. The result was an increase in density and viscosity, as well as in the concentration of sulfur and heavy metals [1]. The depletion of light crude oil resources has led to the exploration of less accessible heavy oil resources that require more processing [A4]. Improved technology, however, has made it possible to access these hard-to-reach resources. In Alberta, 1.9 million barrels of crude bitumen per day were produced in 2012, and that production is expected to reach 3.8 million barrels per day in 2022 [5].

1.2   Current Commercial Extraction Practices

Currently, there are two main methods for extracting bitumen from oil sands: in situ and open-pit mining. The method employed for extraction depends on the distance of the oil sand formation below the earth's surface. Oil sands deposits located more than 75m below the ground are considered too deep for economic mining operations. For such deep deposits, in situ technologies are employed. Two commonly used in situ technologies are cyclic steam stimulation (CSS) and steam-assisted gravity drainage (SAGD). In Cyclic Steam Stimulation, steam at high temperature and pressure is injected into a vertical well in the oil sand deposits. The high-pressure steam creates cracks in the oil sands formation, allowing the steam to penetrate the formation [6]. The heat from the steam reduces the viscosity of the bitumen in the deposit, and both bitumen and condensed steam flow into the vertical well from here they are pumped to the surface, and the procedure is repeated.

In SAGD, two parallel horizontal well are drilled into the base of the oil sand formation. Thermal energy is applied by injecting steam into the upper well, which heats the bitumen, reducing its viscosity, and allowing it to flow to into the lower well where it is pumped to the surface along with the condensed steam [1]. Other in-situ technologies exist like VAPEX process which introduces solvent vapors into the oil sand formation to dissolve bitumen [7] and thermal desorption process that used thermal conduction element to heat up oil sands formation. Approximately 80% of Canada's established crude bitumen reserves are amenable to in situ production [1]. However, bitumen recovery by in situ technologies is typically less than 60% [8]. Efforts to increase the bitumen recovery and the energy efficiency of these processes have led to the employment of a mixture of steam and solvent vapor. However, the loss of the solvent to the reservoir is a major concern [9].

Shallow oil sand deposits, which are no more than 75m below the ground, like those in the Athabasca River basin are processed by open-pit or surface mining followed by hot water extraction using Clark Hot Water Extraction (CHWE) process. In this method, oil sands ore are mined and crushed to reduce the size of the lumps. The crushed ore is then mixed with hot water and caustic soda to form a slurry. The slurry is sent into hydrotransport pipeline during which bitumen is liberated from the sand by attachment to air bubbles entrained during slurry formation [1]. Bitumen is recovered by froth flotation at the extraction plant. The bitumen content of oil sands ore mined in Alberta ranges from 7-14%, and the extracted bitumen (from Athabasca oil sands) has a density of 1029kg/m3 and a viscosity range of 80 -12000 Pa s (at 20°C) [4]. Bitumen recovery from surface mining methods can be as high as 90% [8]. Recoveries, however, are dependent on the composition of the ore deposits, which can have a large variation in bitumen, water, and fine solids contents [4]. In 2014, surface mining operations accounted for 45% of the oil production in Alberta [10].

This research in this study focuses on the bitumen extraction process that follows surface mining procedure.

1.3   Disadvantages of Aqueous Extraction Process

There are several shortcomings of the use of hot water extraction in surface mining operations. First, a large amount of fresh water is consumed in the process. The hot water extraction process use approximately 19 barrels of water to produce one barrel of bitumen [9]. Although the majority of this process water is recycled, some of the water is trapped in unsettled tailings, resulting in a net consumption of 2.1 barrels of fresh water per barrel of oil [8, 11]. Currently, approximately 350 million m^3 per year is withdrawn from the Athabasca River alone [12]. Such

high water consumption has a long-term effect on the river flow and climatic variability of the area [13], which in turn affects the wildlife in the area.

Second, a major byproduct of the hot water extraction process is large volumes of wet tailings produced. These tailings are the most compelling shortcoming of the current extraction process. Mature fine tailings which are a mixture of clay, residual bitumen, and water, require large tailing ponds for storage and accumulated 650 million cubic meters by 2006 [8]. If future bitumen production increases as projected, an estimated 1.8 billion cubic meters of fine tailings would be produced by 2033 [1]. The long settling time for the fine solids means that tailing ponds occupy a large area of land, currently over 77 square kilometers according to the Alberta Government [14]. Consequently, these lands are extremely difficult to reclaim, and they pose a great risk to the wildlife and ecosystem of the area.

Also, chemical contaminants from tailing ponds have been found in groundwater supplies, and neighboring land and air masses indicating the release of these chemicals including carcinogen polycyclic aromatic compounds by leaching or volatilization from the tailing pond [15-18]. There is also the very serious risk of a breach in the wall of the tailing pond and adverse spillage into river supply as was the case in the Obed Mountain Coal Mine incident in 2013 [15]. Such accidents are very expensive to remediate and take a toll on the ecosystem of the area.

Third, owing to the high heat capacity of water, a high amount of energy is required to heat up the water to the temperatures used for bitumen extraction. This energy demand results in a large amount of greenhouse gas emissions from the combustion of fossil fuel to heat water. Nitrogen oxides and sulfur dioxide are the two major emissions of concern in the oil sands operations. Hot water extraction process produces 146 g of nitrogen oxides and 30 g of sulfur oxide per barrel of

bitumen produced [11]. These gases have potential to affect human health and they also cause acid rain [11] that contributes to the degradation of limestone structures, as well as corrosion. Also, nitrous oxide and other emitted gases like methane and carbon monoxide are major contributors to global warming.

Daily bitumen production in Alberta is expected to increase from 1.9 million barrels in 2012 to 3.8 million barrels in 2022 [5]. Under current practice, such a significant increase in bitumen production would not be possible without more fresh water consumption. Any increase in water consumption equates to an increase in all the problems discussed above. As such, the current aqueous extraction process is not sustainable for the future development or the environment. Expansion of oil sands production is beneficial to Canada's economy; however, there is a great need for the development of new technologies to overcome the shortcomings of the water-based process.

1.4   Non-aqueous Extraction Process

The use of non-aqueous extraction technology can significantly decrease water consumption, eliminate tailing ponds, improve energy efficiency and reduce greenhouse gas emission. It also has the potential for high recovery of bitumen. These advantages inspired investigation into non-aqueous bitumen extraction from as early as the 1960s. Coulson used both low boiling hydrocarbons (benzene, toluene, and xylene) and high boiling hydrocarbon (kerosene, coal tar naphtha, petroleum naphtha) to dissolve bitumen in oil sands, before extraction with water [19]. He found both types of hydrocarbon to be effective in reducing the bitumen viscosity, but recommended the use of high boiling, aromatic solvents because of the challenge of loss of low boiling point solvents.

Meadus et al. used naphtha as a solvent for bitumen extraction followed by the addition of small amount of water (at a ratio of 0.1 to the solid) to agglomerate sands and fines particles [20]. The bitumen recovery for the process was over 95%. More recently, Painter et al. experimented with bitumen extraction from tar sands using of ionic liquids (liquid salts) coupled with an organic solvent [21, 22]. The ionic liquid facilitated bitumen separation by destabilizing the bitumen-solid interactions and the process gave a bitumen recovery of over 90%. Although no water was required during the bitumen separation step, it was needed to recover the ionic liquid. Despite the promises of all the above processes, it should be noted that any introduction of water to the extraction process introduced most of the problems associated with the water-based extraction process [23]

Leung and Phillips investigated different solvents including benzene, toluene, and kerosene for bitumen extraction using a rotatory contractor [24]. They found the convective mass transfer of solvent into bitumen to be most critical during the early stages of the extraction process; it occurred up to about 85% extraction, beyond which solvent diffusion into the aggregate became important. They also observed higher mass transfer rate for solvents with high aromaticity or low boiling point. The economics of large-scale bitumen production from oil sands necessitate that the solvent employed for extraction be easy to recover from the extraction gangue. For this reason and also for their odor and toxicity, aromatic solvent like naphtha and kerosene are unsuitable [4]. The ideal solvent for a non-aqueous extraction is one that (i) has a high bitumen solubility to permit high bitumen recovery, (ii) has a low boiling point to enable an easy solvent recovery and (iii) minimizes solid transfer to the bitumen product [25]. Such a solvent would enable the rapid reclamation of mined site as well as meet the pipeline specification for bitumen transport [4].

Wu and Dabros investigated the performance of light hydrocarbons (pentane, heptane, cyclopentane, a mixture of pentane and cyclopentane) and toluene as solvents for non-aqueous extraction of oil sands followed by centrifuge filtration or pressure filtration [25]. They concluded that cyclopentane was the best solvent given its high bitumen recovery of 90% and a lower residual solvent content in the extraction tailings. Hooshair et al. studied the water-free extraction of high and medium grade oil sands ores using mixtures of toluene and heptane [8]. Bitumen recoveries of over 96% were obtained for both grades of ore and all solvent mixture. Nikakhtari et al. followed similar protocol for water free extraction of rich-grade Alberta oil sand sample using a range of solvents, including aromatics, cycloalkanes and biologically derived solvent [26]. They recommended cyclohexane as a suitable solvent for non-aqueous extraction based on a high bitumen recovery, low fines content of the recovered bitumen, and rapid removal rate of cyclohexane from the extraction tailings (gangue). This fast evaporation rate and high recovery of bitumen could be attributed to cyclohexane's high vapor pressure and high solvent power [9], a characteristic of most cycloalkanes. The almost dry gangue produced from extraction could be returned to the mined site immediately, enabling the quick reclamation of the area [9].

The process by which solvents dissolves bitumen in oil sands can be considered as a mixing process between solvent and solute [23]. According to the Hildebrand solubility theory, a solute is soluble in a solvent when the mixing enthalpy is small, in which case the solute and solvent has similar solubility parameter [23]. The stability of asphaltene, the least soluble component of bitumen, can be correlated with the Hildebrand solubility parameter (δ). Cyclohexane ($\delta = 16.8 MP1^{/2}$) [27], as well as other solvents like toluene and cyclopentane that dissolve bitumen without precipitating asphaltene, has a solubility parameter close to that of asphaltene

(δ=16.2MP1$^{/2}$ for Athabasca bitumen [3]). As such, bitumen extraction with these solvents can be achieved without the need for energy input. Richard et al. [28] quantitatively showed that the minimum energy requirement to remove cyclohexane from the extraction gangue of range of oil sands samples could be achieved at ambient temperature and atmospheric pressure. Clearly, the use of cyclohexane as a solvent for non-aqueous extraction of bitumen from oil sands has great potential. Figure 1 shows a summary of the process for extracting bitumen from oil sands using non-aqueous organic solvent
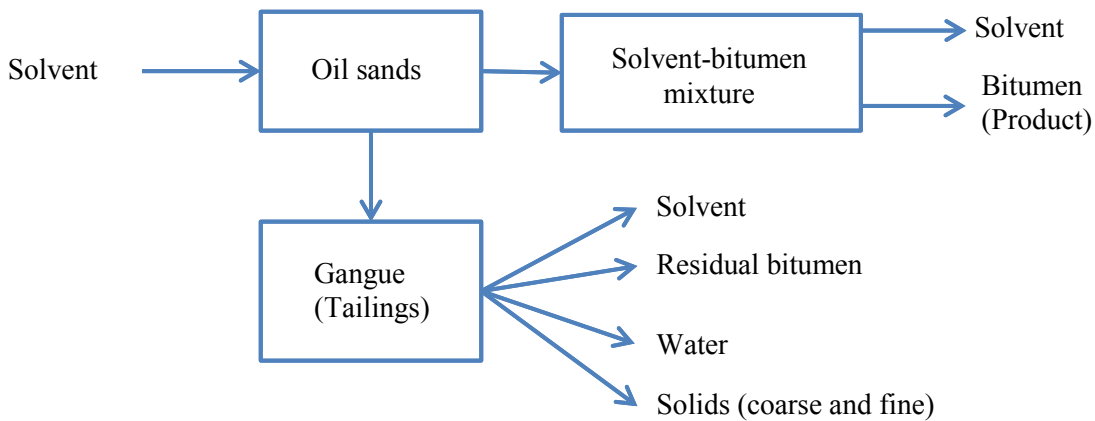
Figure 1: Non-aqueous extraction of bitumen using organic solvent

Although results from these studies have been promising, solvent extraction has yet to be employed on a commercial scale for bitumen extraction. The biggest technical, economic and environmental challenge to the commercialization of non-aqueous extraction technologies is the recovery of solvent from the gangue [29, 30]. There are four main components of the extraction gangue: the excess solvent, residual (unrecovered) bitumen, water, and solids. Nikakhtari et al. [16] showed that essentially all the water originally present in the oil sands ore is retained in the gangue during cyclohexane extraction. The gangue solids consist of coarse solids and fines

solids, similar to the original ore, but with less the amount of fine solids that migrated into the bitumen product.

Recent research has examined how various factors affect the recovery of cyclohexane from the gangue. Richard et al. [28] studied the effect of temperature and pressure on cyclohexane recovery from extraction gangues of rich-grade and low-grade ores. They performed experiments on a packed bed of sample in a tin dish in a controlled oven under different combination of temperature and pressure while also measuring the evaporation of cyclohexane. Increasing temperature and decreasing pressure were found to increase the mass flux of cyclohexane in both gangue samples. Also, the cyclohexane evaporation flux for low-grade gangue was lower than that for the rich-grade gangue. They attributed this to the high water and fines content of the low-grade gangue. Furthermore, they observed the migration of residual bitumen which formed dark bitumen-enriched top-layer in the rich-grade gangue. Siddhant et al. [31] studied the effect of the residual bitumen and initial cyclohexane content on evaporation of cyclohexane from the gangue. They developed a protocol to make controlled sample (reconstituted gangue) in which the gangue composition could be varied. Reconstituted gangues of a range of bitumen content (0.5-2%) and cyclohexane content (8 -12%) were prepared to study the effect of these variables. The range of components selected for reconstituted gangue corresponded to those obtained in rich-grade gangue and the samples were representatives of the extracted gangues. Higher residual bitumen led to a lower cyclohexane removal flux. This observation was attributed to a decreased sorptivity arising from the increased viscosity associated with bitumen dissolution in cyclohexane. In fact, there was a bi-directional mass transfer that occurs between cyclohexane and bitumen [32], which contributed as well to the higher residual solvent content after drying. The bitumen enrichment that occurred was thus higher for samples with lower residual bitumen

content than high ones. The initial cyclohexane content was observed to increase the rate of cyclohexane removal as 12% cyclohexane sample had a higher initial evaporation flux than 8% samples.

Nikakhtari et al. studied the effect of relative humidity, temperature and water addition during extraction on the extent of cyclohexane removal from cyclohexane-extracted oil sands gangue [33]. They found two constant drying stages, one dominated by cyclohexane removal and other by water removal. The initial cyclohexane-dominated drying stage was unaffected by changes in relative humidity. The observation on the increased solvent removal with increasing temperature was in agreement with Richard et al. [28]. The addition of water before oil sands extraction with cyclohexane was found to decrease cyclohexane mass flux from the gangue by forming barriers to evaporation [33].

In the oil sand industry, it is recognized that coarse solids do not cause any problems in either aqueous or non-aqueous extraction processes [8]. On the contrary, fine solids particularly clay minerals are known to detrimental in water-based bitumen extraction [8]. Here, clay reduces bitumen recovery by slime coating of bitumen droplets [1]. Bi-wettable clay particles (Janus particles) in oil sands can attach to the surface of bitumen droplet during hydrotranport, preventing the attachment of hydrophobic air bubbles, which is necessary for bitumen recovery during froth flotation. In general, bitumen recovery decreases with increasing fines content, even when the pH of the process water is adjusted near the optimum [34]. Hydrophobic fines migration into bitumen also reduces the quality of the product bitumen in aqueous extraction. The higher the fines migration into the bitumen product, the greater the effort and cost required to remove the solids, to meet pipeline specifications for transport. Fines also play a major role in tailings management. Clay contributes primarily to mature fine tailings (MFT) in tailings ponds,

making up 13% of MFT. These fine and ultrafine particles remain dispersed in the water, which if left untreated, would take decades to settle [1]. As stated earlier, this is a major problem because of the difficulty in reclaiming land.

In non-aqueous extraction, fine solids also migrate into the product bitumen because of their hydrophobicity [35]. The amount of fine solids migrating to the product is sensitive to the oil sands ore grade. Nikakhtari et al. [35] found that the extent of fines migration into the bitumen product is dependent on the water and the fine solids content of the ore. They demonstrated that fine solids migration is far more sensitive to the water content, and the removal of water from the ore lead to more fines. Connate water was found to plays a crucial role in binding and retaining the fine solids in the extraction gangue because its removal by drying lead to an increase in the release of the solids. High fines content in the bitumen lowers the quality of the product and increases the cost of production due to addition work required to remove the fines.

Although fines solids migrate into the bitumen product in NAE process, the majority of the fines in the ore are retained in the extraction gangue [35]. Much less is known about the role on fine solids in the extraction gangue, although they are thought to contribute to the poor recovery of non-aqueous solvents from the extraction gangue [8]. To the best of our knowledge, no studies are available in literature on the role of fine solids on the recovery of solvent from non-aqueous extraction gangue. The majority of the closest works are studies on volatile organic compounds (VOCs) in agricultural soil, and these were predominately aromatic VOCs in the gaseous phase [36, 37]. They do however suggest a higher adsorption capacity of clayey soil towards VOC.

Yu et al. [32] showed that the residual solvent content of gangue from solvent extracted oil sands ore increased about 50% when the median particle size of the ore decreased from 1335um to

125um. However, they also acknowledge the significant contribution of residual bitumen, (which was higher for the smaller sized particle) to this reduction. Additionally, they did not examine the wettability of the particles. Pore size distribution and wettability have been shown to play a key role in the drying of water from packed bed [38]. Little literature exists on their influence on the drying of light aliphatic hydrocarbons.

1.5 Drying Mechanism

Before analyzing the evaporation of solvent from non-aqueous extraction gangue, it is essential to develop a deep understanding of the mechanism of solvent removal from porous media. While limited literature exists for the drying on two immiscible solvents like cyclohexane and water in a solid matrix, the numerous studies on the drying of water from porous media can provide insight into the drying process for the solvent.

A porous media can be described as a network of pores connected by throats to form capillaries [39]. Drying in porous media is considered to be a drainage process in which air replaces an evaporating liquid that recedes into the pores [39]. The drying process is described by invasion percolation in which the next throat to be invaded by air is the one with the largest size i.e. smallest capillary threshold [40, 41]. When gravity or viscous forces are significant, the displacement process is described by invasion percolation in a stabilizing gradient [40,41]. For a long while, drying of porous media was believed to occur primarily through a direct vaporization of the liquid and transfer by diffusion and convection out of the porous media. Further understanding of the drying process came with works accounting for viscous effects [42], gravity effect [43], advection and transients in the gas phase [41], and temperature gradient [44] on the evaporation. However, none of these could explain the six-fold higher drying rates in experiment compared to simulation observed by Laurindo and Prat [31]. The high drying rate was attributed

to liquid films that maintain hydraulic conductivity to the surface. Fluid flow through liquid films that form in the cavity of pore wall as the liquid-gas menisci recedes into the pore [45], and this is a dominant mechanism in the drying of porous media [43].

Liquid films exist because pores networks do not have cylindrical geometry [40]. In realistic (square) pore geometry, liquid films form along corners of pore surface as the liquid-air meniscus recedes in the pore space [40], as depicted in Figure 2.
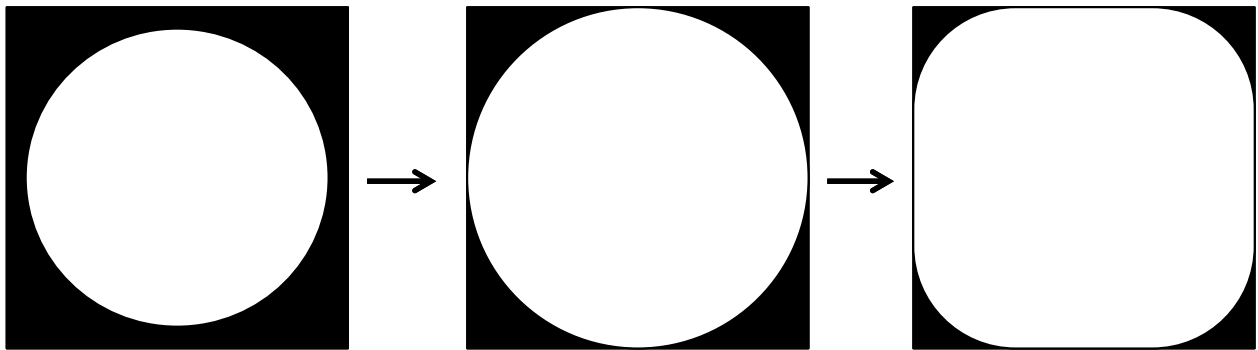
Figure 2: Formation of liquid film at the corners of pores with square geometry

Yiotis et al. provided a distinctive representation for the evaporation of liquid from a porous media [40]. They depicted a 2D square lattice of pores connected through throats in a medium and in which mass transfer and fluid flow out of the medium only occurs through one end (of the lattice) that is exposed to flowing air at ambient temperature. Figure 3 is a pictorial representation of such a lattice.
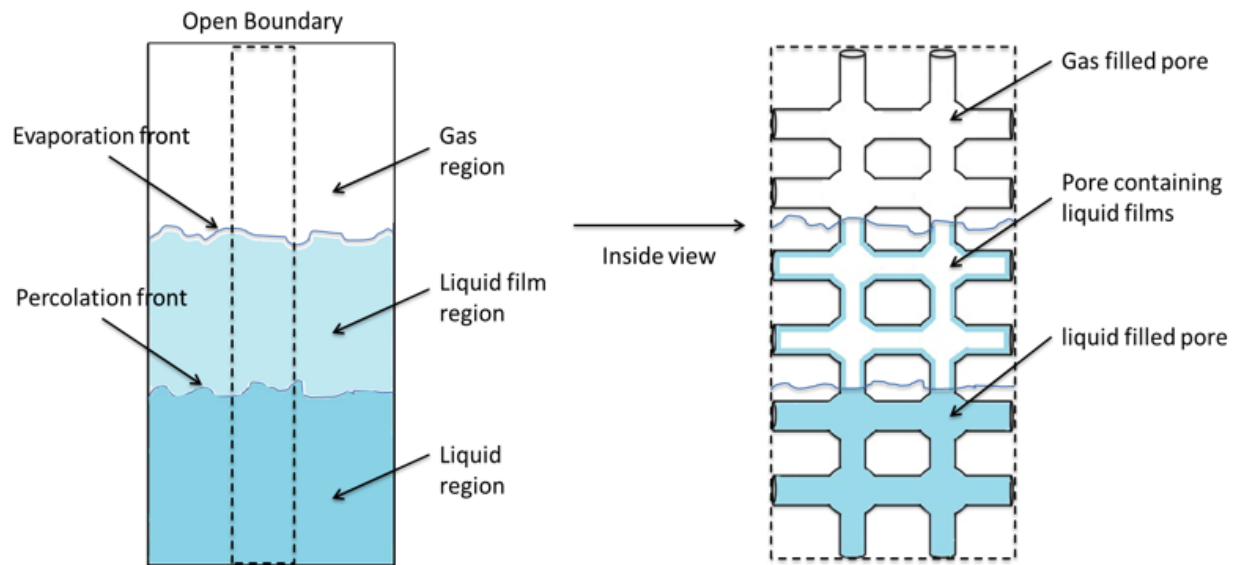
Figure 3: Regions and pore types present during the drying of a wetting fluid from porous media.

The drying process entails four different regions:

(i)   a liquid region that initially covers the entire domain and contains only liquid saturated pores ;

(ii)   a film region with pores occupied by gas but which also contain liquid films;

(iii)   a complete dry gas region with pores containing diffusive gas; and

(iv)   an open region at the external surface of the porous media [46].

The interface between the liquid region and film region forms the percolation front, while that between the film region and the dry region acts as the evaporation front [46].

For a saturated porous media, the initial stage of drying exhibits a constant evaporation rate and is known as the constant rate period (CRP) or Stage 1 evaporation. During this period, the external surface of the porous medium remains partially saturated for an extended period as

liquid film maintain liquid continuity from the receding percolation front to the surface [46]. Surface saturation decrease over time as viscous and gravity effects increase [44, 46]. As long as liquid films remain connected to the external surface, the partial pressure of the evaporating liquid at the surface remains constant and equal to the vapor pressure of the liquid given a thickness of the external mass transfer layer that is significantly larger than the characteristic pore size of the medium [48]. Hence, Stage 1 evaporation is controlled by external mass transfer [46].

At a critical film length when viscous and gravity effects exceed capillarity, the films detach from the external surface of the medium [46]. Film tips acting as evaporation fronts recede further into the pores, leaving behind an increasingly completely dry region of pores below the surface of the medium [46]. Mass transfer occurs through vapor diffusion in this dry region of the porous media and the mass boundary layer above the porous media. Due to porosity and tortuosity, the effective molecular diffusivity of the liquid vapor in the porous media is much lower than the effective diffusivity in the mass boundary layer [46]. In other words, the rate of internal mass transfer is always lower than the rate of external mass transfer. Consequently, the evaporative mass flux during this stage of drying is limited by the slow internal vapor diffusion through the porous media. As drying continues and the drying front recedes further into the porous media, resistance to internal mass transfer progressively increases, resulting in a continuous decrease in the drying rate [46]. This period is called the falling rate period (FRP) or Stage 2 evaporation.

The extent of the liquid film is determined by the balance between capillary force and counteracting gravitational and viscous dissipation [49]. The relationships between these forces are described by dimensionless numbers: the capillary number, Ca_f defines the ratio of viscous

15

forces to capillary forces in the film, and the bond number, Bo expresses the ratio of gravity to capillary forces [46]. There is also the Sherwood number, Sh, which describes the external mass transfer that occurs at the surface of the porous media [46]. Increasing Ca_f and Bo indicate more significant effects of viscous dissipation and gravity respectively. The Sherwood number increases as external boundary layer becomes thinner

Flow within liquid films is driven by capillary induced pressure gradient [45]. Capillary flow in porous media occurs as a result of capillary force, which in the simple capillary tube such as those in Figure 4 is a balance between cohesive forces within the liquid and adhesive force between the liquid and the tube wall, which cause the liquid to rise in the tube.
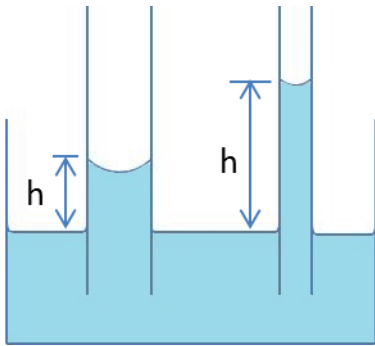
Figure 4: Liquid rise in capillary tubes.

For drying condition, flow is driven by capillary pressure, which is the pressure difference between the liquid in the pore and gas phase above it. The Young-Laplace equation gives the pressure difference (ΔP) for a curved liquid surface

$$\Delta P = \gamma \left(\frac{1}{R_1} + \frac{1}{R_2} \right) \qquad\qquad Equation\ 1$$

where γ is the interfacial tension, R_1 and R_2 are the principal radii of curvature of the liquid-gas interface. For capillaries, like those in Figure 4,

$$\Delta P = \rho g h \qquad\qquad Equation\ 2$$

and equation 1 becomes

$$P_c = P_g - P_l = \frac{2\gamma cos\theta}{R} \qquad\qquad Equation\ 3$$

where P_c is the capillary pressure, P_l is the pressure of the liquid phase, P_g is the pressure of the gas phase, γ represents the interfacial tension between the liquid and air, θ represents the contact angle between the liquid and the pore wall, and R is the pore radius. Equation 2 above shows that the capillary pressure depends on the surface tension of the liquid, the wettability of the pore solid by the liquid and the size of the pore. Wettability describes the preference of a solid to be in contact with one liquid over another [50] and is indicated by the contact angle [51]. Contact angle between 0° and 90° indicates that the liquid wets the capillary walls, and meniscus formation results in a suction pressure that causes the liquid to rise in the capillary [28]. Pore size also affects capillary pressure. As shown by equation 2, a small capillary tube gives rise to a higher the capillary pressure and consequently, the wetting liquid will rise higher in the capillary.

During the drying of a wetting fluid, a characteristic length provides a measure of the strength of a capillary force and can often be deduced by the pore size distribution of a porous medium [52]. The characteristic length is defined as the drying front depth (the distance between the receding saturated zone and the evaporating surface) or the length of the film region at which hydraulic connectivity to the open surface is broken [47]. This point occurs when capillary forces are

balanced out by gravity and viscous resistance [52] and marks the end of stage-1 evaporation and the onset of the slower, diffusion- dominated stage-2 evaporation [47].

Liquid films are negligible in porous media when the evaporating fluid in non-wetting [53]. Shokri et al. observed that hydraulic connectivity required to sustain Stage 1 evaporation could not form in the drying of water from a hydrophobic porous medium; rather, vapor diffusion supplied the evaporative demand from the hydrophobic medium [52]. When hydrophobic particles when mixed with hydrophilic ones in a porous medium, water migrated in films formed along hydrophilic particle while air invaded domains around hydrophobic particles [40]. In the drying of a dye solution in porous media with a vertical contrast of hydrophobic and hydrophilic particles, low capillary pressure led to the hydrophobic side being preferentially invaded by air while evaporation occurred only on the hydrophilic side as evidenced by the deposition of dye on that side [53]. These studies demonstrate that the significance of wettability in the drying process since the introduction of hydrophobic particles can weaken the capillary forces in the pore structure in the drying of a hydrophilic liquid or vice versa.

1.6   Objective

The goal of this research is to investigate the role of fine solids on the recovery of cyclohexane from the gangue of non-aqueous extraction process. In the process, we will examine the contribution of the two major attributes of fines solids, wettability, and particle size distribution and how they affect evaporation of cyclohexane from packed bed of gangue under ambient conditions

2 Methodology

2.1 Materials

The oils sands used in this study was provided by Syncrude Canada Limited. Both rich-grade and low-grade ore from the Athabasca oil sands deposit were used. For solvents, toluene was used for Dean-Stark extraction, cyclohexane was used for non-aqueous bitumen extraction, and methanol was used for film flotation. All three solvent were Certified ACS grade, supplied by Fisher Scientific, Canada.

Oil sand samples were received in large containers. They were then milled to homogenize the sample, and 1.5 kg subsamples were stored in a deep freezer at -13°C. The samples were first thawed overnight at room temperature before use.

2.2 Dean-Stark Extraction

Dean-Stark extraction was used to determine the bitumen, water, and mineral solids content of the oil sands sample and to isolate mineral solids for further experiment. Approximately 100g of the sample was weighed into a thimble. The thimble was placed in a wire holder, which was then suspended in the neck of a round-bottom flask, from an adaptor. The adaptor connected the round-bottom flask, containing approximately 250ml of toluene to a condenser, which was equipped with a graduated trap. Cold water flowed through the condenser to condense both solvent and water vapor. Vaporized toluene refluxed through the sample and dissolved bitumen which collected in the flask. Connate water from the ore vaporized, condensed and collected in the trap, while mineral solid remained in the thimble. A typical Dean-stark procedure requires 3-

4hrs. However, our extractions left to run overnight to ensure complete removal of bitumen, thus producing bitumen-free mineral solids that were used for other experiments.

2.3 Pycnometry

The particle density of the oil sand mineral solids was determined by pycnometry. Approximately 4 g of the bitumen-free solid (dry soxhlet gangue) was weighed into a preweighed 10 ml volumetric flask. The flask was then filled to mark using cyclohexane. The flask was shaken to release trapped air bubbles and then left overnight for the solvent to invade pores of the mineral solids. It was then re-filled to mark and weighed to get the weight of the solid and solvent. The particle density was calculated as the mass of the solids in the flask over the volume occupied by the solids [54].

2.4 Non-aqueous Extraction Procedure

The procedure for non-aqueous bitumen extraction is shown in Figure 5, and it was based on previous work done by Nikikhtari et al. [26]. The extraction was carried out at room temperature (22±1°C) and ambient pressure, and the procedure is described as follows: 150 g of oil sands and 100 g of cyclohexane were added to a 500 ml Teflon jar. The jar was sealed and rotated on a rotary mixer (rotator drive STR4, Stuart) at 60 rpm for 10 mins. The digested oil sand slurry was transferred to a graduated cylinder to sediment for 30 mins. The top layer, (1st supernatant) was separated from the bottom layer by siphoning. The sediments in the cylinder were transferred back into the Teflon jar, and 50 g of solvent was added for a second digestion. The mixture was rotated using the rotary mixer for 10 mins at 60 rpm. The oil sands slurry was sieved using a 45 μm aperture 8" diameter sieve (ASTM E-11 Standard test sieve no. 325, Fisher Scientific Co., Waltham, MA) while vibrating for 5 mins. The liquid that passed through the sieve was the called the second supernatant. The solids retained on the sieve were washed with two batches of

50 g of solvent while vibrating for 5 mins during each wash. The third supernatant was collected as the combined liquid from the two wash steps. The solid remaining on the sieve after the extraction was the extraction tailing or gangue. A small subsample of the gangue was obtained, and the rest were immediately transferred into glass jars and capped, sealed and stored at -13°C in a freezer. The first supernatant was transferred into 250ml Teflon bottle and centrifuged at 3000 RCF (relative centrifugal force) for 1 hour using an Avanti J-301 centrifuge (Beckman Coulter, Mississauga, ON) with a JA-10 rotor. Similarly, the second and third supernatants for each sample were combined and centrifuged to separate fine solids present in the product. The bitumen-solvent mixture after centrifugation was decanted off and the centrifuged solids, together with subsamples of the gangue were dried in a vacuum oven at 70°C for 24 hours and stored for later analysis. A Karl Fischer titrator (Mettler DL18) was used to determine the water content of the bitumen-solvent supernatant.
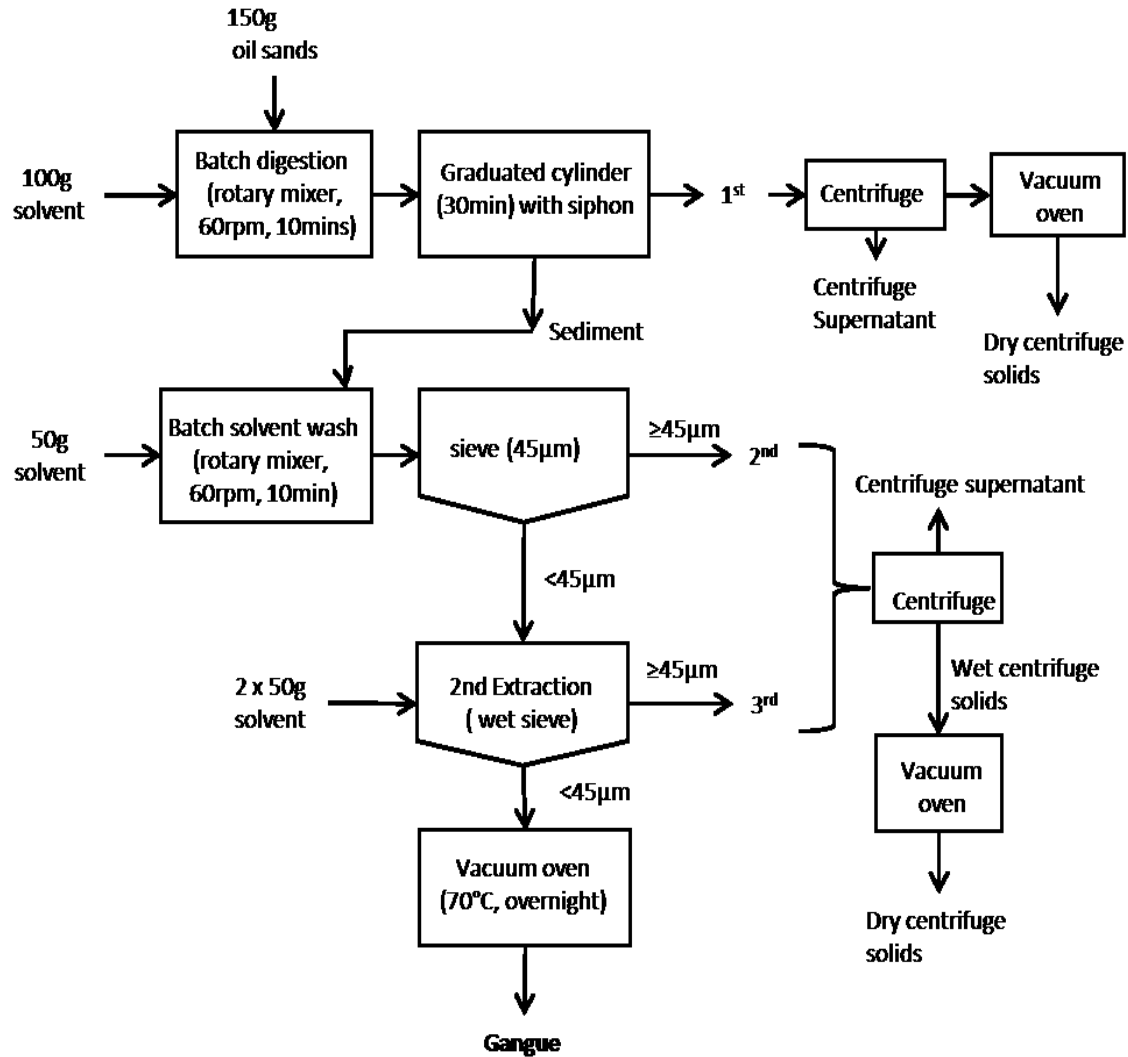
Figure 5: Flow diagram for non-aqueous extraction process

2.5 The Requirements for Reconstituted Gangue

As mentioned earlier, the gangue produced in the non-aqueous extraction contains some solvent, residual bitumen, water as well as both coarse and fine solids. The solvent in the gangue can be recovered by drying of the gangue. Recovery of the solvent is important to the economics of the NAE process. Each batch of non-aqueous extraction of an oil sand ore produces a gangue of different composition of solvent, residual bitumen, water and fine solids. This variability creates a problem when analyzing the gangue as it becomes difficult to pinpoint the effect of its

22

constituents on the drying process. Any systematic study of a process requires clearly defined parameters for accurate analysis. Hence, making a synthetic or reconstituted gangue would allow us to control the composition of the gangue, enabling us to elucidate the effect of each component on the drying process.

Given the challenges of creating reconstituted gangue [28], our target in this study was not necessarily to create an exact duplicate of the extracted gangue; rather, it was to create a sample that approximates the drying behavior of the extracted gangue and acts as a substitute whose composition can be controlled.

2.6   Composition of the Reconstituted Gangue

The reconstituted gangue was made up of the same constituents as the extracted gangue. Clean soxhlet extracted sands (soxhlet gangue) from the Dean-stark extractions were collected after drying and used as the base material for making the reconstituted gangue as shown in Figure 6. The target bitumen content for the reconstituted gangue was determined from the range of residual bitumen content in the extracted gangue. The bitumen content of each extracted gangue was evaluated from the bitumen associated carbon or bitumen carbon (Bit.C) % of the gangue. Bit. C % was calculated as the difference between the wt % carbon content of the dried gangue (due to bitumen and toluene insoluble carbon) and the carbon content of the soxhlet extracted sand (toluene insoluble carbon) obtained from CHNS analysis. Details of this calculation can be found in Appendix A. The range of bitumen carbon content for low-grade gangue in weight % was 2.0-2.4 wt % Bit.C, which was equivalent to 2.4 -2.8 wt % bitumen, based on a carbon mass fraction of 0.833 found in bitumen [55, 56]. This carbon content of pure bitumen was also confirmed by our CHNS analysis.

The target cyclohexane content for the reconstituted gangue were 12 wt % and while that for water was 10 wt % (solvent free weight basis). Both cyclohexane and water content were based on the mean values obtained from Dean-Stark extraction of the extracted gangue.

2.7   Preparation of Reconstituted Gangue
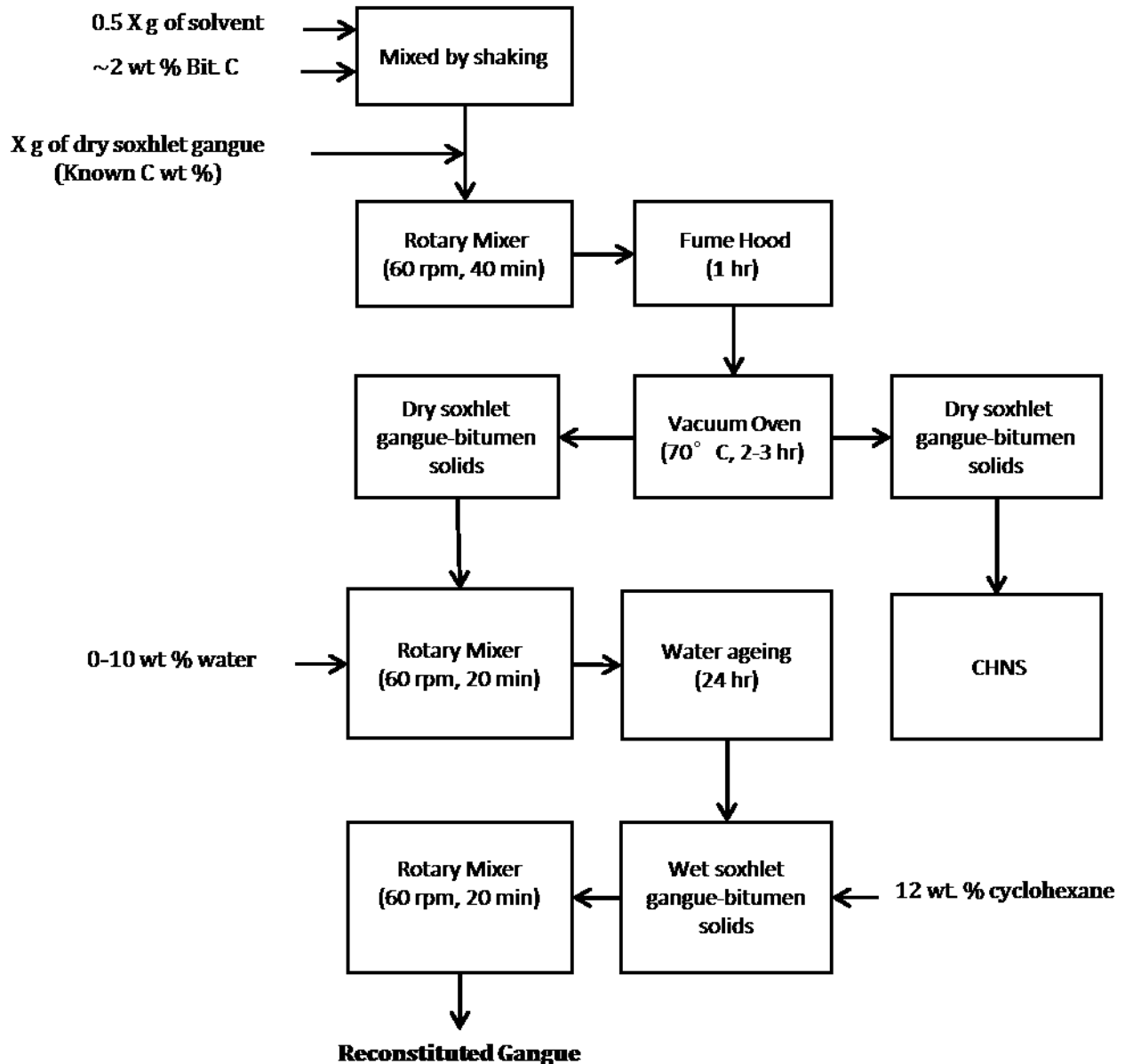
Figure 6: Protocol for making reconstituted gangue

Soxhlet gangue, obtained after exhaustive toluene extraction of oil sand ore was used in the preparation of reconstituted gangue. The gangue was dried for 24hrs at 70°C in a vacuum oven to remove all toluene left in the pores after Dean-Stark extraction. The fine and coarse solids composition of Soxhlet gangue was taken to be approximately the same as that of the extracted gangue. This approximation was justified based on the fact that the maximum amount of solids (fines) migrating into the bitumen product was less than 1% of the total oil sands solids during the bitumen extraction. The carbon content of the dry soxhlet gangue obtained by CHNS analysis was attributed to toluene-insoluble carbon. Bitumen is highly soluble in toluene; thus, given the exhaustive nature of the toluene extraction performed, all bitumen associated carbon was expected to have been removed. Also, we observed that the low-grade soxhlet gangue obtained from Dean-Stark extraction formed clumps due to the higher water content of the low-grade ore. To facilitate the reconstituted gangue preparation, these clumps were broken up by mild grinding of the ore. McKenzie et al. suggested that mild grinding does not change particle size distribution process [57]. The results from particle size distribution analysis confirmed that there was no significant change in the particle size distribution of the soxhlet gangue from breaking up lumps. The reconstituted gangue was prepared using cyclohexane as a solvent in 500 ml capped-Teflon bottles.

2.7.1 Addition of Bitumen

50-200 g of Soxhlet gangue was used per batch of reconstituted gangue prepared. An amount of cyclohexane equivalent to half the weight of Soxhlet gangue to be used was added to a pre-weighed amount of bitumen in a 500 ml Teflon jar. The mass of bitumen added was calculated based on the final target Bit. C % in the reconstituted gangue. As such, this amount also depended on the amount of starting Soxhlet gangue used. After the addition of cyclohexane to

bitumen, the jar was capped and shaken until the bitumen completely dissolved in the cyclohexane. The dry soxhlet gangue was added to the jar, and the combination was then placed on a rotary mixer for mixing at 60rpm for 40mins. It was not practical to mix all three constituents (soxhlet gangue, cyclohexane, and bitumen) all at once due to the high component ratio that would be required and also because of the non-uniform mixing that would result from such high ratios [31]. This procedure used required Soxhlet gangue to cyclohexane-bitumen solution mixing ratio of only 2:1, enabling proper mixing and slurry formation [31]. The slurry was transferred into a large Pyrex glass crystallization dish and swirled and stirred continuously for 1 hr to ensure uniform bitumen distribution while also removing cyclohexane. This process prevented bitumen from migrating within the solids as would happen if the slurry was left unattended. This procedure, as well as all preceding step in the bitumen addition, were performed in the fume hood for safety and also to facilitate cyclohexane evaporation with airflow in the fume hood during the solvent removal step. After one hour, the glass dish with soxhlet gangue-bitumen solids was placed under vacuum in an oven at 70°C for 2-3hrs to complete drying and to remove leftover cyclohexane from the pores of the solid. The dry bitumen coated solids obtained at the end of this process is dry soxhlet gangue-bitumen solids, which we refer to as DSBS in the rest of this paper. A subsample of the DSBS was taken for elemental analysis on the CHNS analyzer.

2.7.2 Addition of water

A known amount of DSBS was transferred into a clean Teflon bottle. The target wt % of water was added to jar based on the weight of DSBS in the jar. The Teflon jar with its content was capped and placed in the rotary mixer for mixing at 60rpm for 20mins. After mixing, wet soxhlet gangue-bitumen solids (WSBS) were obtained. The Teflon jar was sealed using Parafilm to

prevent water loss during the aging process. The aging process involved let the WSBS stand for 24hrs. The procedure for water addition as described here was designed to replicate the dispersion of water in the gangue that occurs during the extraction process [31].

For reconstituted gangue samples prepared without the addition of bitumen, lumps were observed to have formed after mixing dry soxhlet gangue with water for low-grade samples. The lump formation was attributed to the aggregation of fine solids by water. A spatula was used to break up these lumps and mix up the wet soxhlet gangue before and after water aging.

2.7.3 Addition of cyclohexane

After water aging, the mass of cyclohexane required to attain final target cyclohexane wt %, which was dependent on the mass of the WSBS is added to the Teflon jar. The jar was capped and sealed with parafilm and then placed on the rotary mixer for mixing at 60 rpm for 20 mins. After about 10 mins of rotation, the jar was opened and any lump formed was broken up using a spatula and mixed up. The sample was then resealed and rotated for the remaining 10mins. The reconstituted gangue sample was obtained after the rotary mixing, and it was immediately transferred to a pre-label glass jar and capped and sealed with parafilm. The reconstituted gangue samples were stored at -14°C in a freezer (to minimize solvent loss) until ready to use.

Using the above protocol, we prepared different samples ranging from reconstituted low-grade gangue containing similar composition as low-grade extracted gangue, to low-grade gangue containing no bitumen. Rich-grade reconstituted gangue containing no bitumen was also prepared using the similar protocol [31].

2.8   Sample packing

Approximately 25.0 ± 0.5 g of the sample was weighed into a 5cm inner diameter, 1.5cm deep glass petri dish. (CLS316060, Pyrex®). The sample spread out evenly to a 1.00 ± 0.05 cm bed height. By keeping the sample mass, bed height and bed radius constant, we were able to keep the bulk density and average porosity of the bed constant. The bulk density and average porosity for low-grade bitumen containing samples (which also had higher water content) were 1.00 ± 0.02 g/cm^3 and 0.60 ± 0.01 respectively, while those for both rich-grade and low-grade bitumen free samples were 1.09 ± 0.02 g/cm^3 and 0.57 ± 0.01 respectively. These were based on a particle density of 2.53 ± 0.01 g/cm^3 for both rich-grade and low-grade soxhlet gangue. The bulk density for each packed bed was calculated by dividing the mass of the solid in the bed by the volume occupied by the bed, which is given by equation 4

$$Bulk\ density = \frac{mass\ of\ solid\ in\ packed\ bed}{Volume\ of\ packed\ bed} \qquad \qquad Equation\ 4$$

The average porosity was calculated using equation 5

$$Porosity = 1 - \frac{\rho_{bulk}}{\rho_{particle}} \qquad \qquad Equation\ 5$$

28

2.9 Drying Experiment
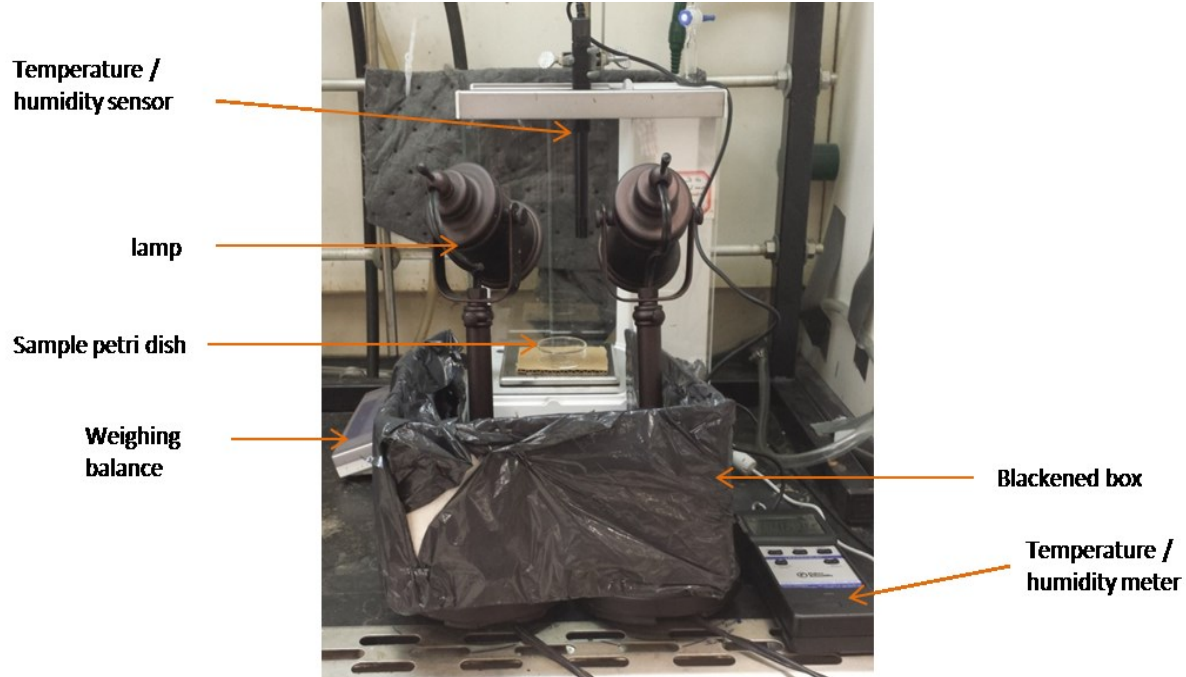
Figure 7: Set up for drying experiment

Before each drying experiment, the sample was removed from the freezer and allowed to thaw before sampling. After thawing, the sample was mixed manually with a spatula to homogenize the samples, before weighing and packing. A timer was used to record the time taken to thaw, weigh and pack the sample. The weights of the petri dish before and after packing were also recorded. Figure 7 shows a set up for the drying experiment. After packing, the sample is immediate transferred to the fume hood and placed on the balance (Model XP203S, Mettler Toledo, Mississauga, ON) capable measuring weights to 0.001g. This balance was connected to a laptop that recorded the weight approximately every 20s, using Mettler Toledo software.

The top of the balance was kept open, and the probe of a dual temperature-humidity meter was suspended at a height above the sample of about half the height of the balance. Both temperature and relative humidity were monitored and recorded manually at intervals during the experiment. The front door of the balance was also kept open to allow air flow through the balance. The sash

height of the fume hood was kept at a level to ensure a flow rate of 100-120 fpm, which gave measured air flow rates of V_x = 0.03-0.08 m/s and V_y = 0.01-0.04 m/s over the sample in the balance. Two lamps and a blackened cardboard box were used to illuminate the sample and reduce reflection during video recording following the procedure outlined in Siddhant et al. [31]. However, these were only employed in the first half of experiments (i.e. for runs involving bitumen).

All drying experiments were conducted at room temperature (22±1°C). The samples were allowed to run for 2-4 hours, sufficient time to remove most of the cyclohexane in the gangue. Four hours was required for the drying of low-grade extracted and reconstituted gangue containing bitumen and high water content (10 % water) while two hrs was sufficient to dry rich-grade and low-grade gangue containing no bitumen and 0-3.7 %* water. There was fluctuation in the recorded weight of the experiment due to air currents. This error in the balance weight before and at the end of the experiment was recorded and factored in during analysis.

 At the end of each experiment, the sample was transferred to a different balance (Model AB265-S, Mettler Toledo, Mississauga, ON) and the weight recorded again. For samples containing bitumen, bitumen migration resulted in a bitumen-enriched top layer and bitumen-deficient bottom layer. For these samples, the top and bottom layers were separated and analyzed separately. For bitumen-free samples, each sample was mixed quickly with a spatula before subsampling for cyclohexane analysis. Approximately 5 g subsamples were transferred directly into pre-weighed glass sample tube. The sample was held in place in the glass tube between glass wool plugs, and the tubes were sealed with parafilm. The sample was then stored in the freezer for 30mins to minimize loss of cyclohexane before analysis.

2.10 Residual cyclohexane analysis using QICMS

Analysis of the residual cyclohexane content of the samples was done using a thermal sample collection apparatus (Short Path Thermal Collection System, Scientific Instrument Services Inc., Rigoes, NJ) connected to Quartz Inert Capillary Mass Spectrometer (HPR 20 QIC R & D, Hiden Analytical, Warrington, England). The glass tube containing the sample was placed inside the thermal desorption unit which operated at 21- 60°C. A high purity nitrogen carrier gas (Ultra High Pure 5.0, Praxair, Canada) connected to one end of the glass tube, carried desorbed gas to the mass spectrometer, at a flow rate of 18 ± 1ml/min. The mass spectrometer was maintained at a pressure of 2×10^{-6} torr for the duration of the cyclohexane analysis. Prior to analyzing the samples, the mass spectrometer was calibrated by injecting known volume of cyclohexane directly into 5g of clean soxhlet gangue packed in glass sample tubes. Following the desorption on the thermal unit and analysis on the mass spectrometer, a calibration curve was obtained by plotting the peak integral vs. the injected volume of cyclohexane. The solvent concentration in ppm was obtained after factoring in the mass of the soxhlet gangue. A MATLAB script based on the calibration curve data was developed by Siddhant et al. [31] and it produced the residual solvent concentration in parts per million (ppm) for each sample from peak integral value and mass of sample analyzed.

2.11 CHNS Analysis

An elemental analyzer (Flash 2000 CHNS/0 Analyzer, Thermo Scientific) was used to determine the total carbon, hydrogen, nitrogen and sulfur content of the oil sand ore, extracted bitumen, dry soxhlet gangue from Dean-Stark extraction, as well as the dry extracted gangue and reconstituted gangue.

Before analysis, each sample was dried for 24hrs under vacuum in an oven at 70°C. The samples were then homogenized by grinding using a marble mortar and pestle. 12-15mg of each sample was weighed out in aluminum dishes. The dish was then crumpled with tweezers to lock in the samples before loading in the autosampler of the analyzer. After loading, the samples were sequentially sent into a reactor where they were catalytically combusted at about 1800°C [58]. The products of the combustion (CO_2, H_2O, N_2 and SO_2) were fed into a chromatographic column for separation before being passed into a thermal conductivity detector. The analyzer gave results of the elemental composition in wt % by correlating thermal conduction of the respective gas to peak heights of each gas obtained from known reference materials. The carbon content obtained were used in the calculating the bitumen-associated carbon content and as well as for bitumen recovery calculation. 3-4 subsamples of each sample were analyzed, and the average result was used in the calculation. The overall time for each sample analysis was about 12 mins

2.12   Fine solids analysis

Fine solids were extracted from the dry soxhlet gangue by wet sieving. Figure 8 shows the flow diagram for the fine extraction procedure. First, 50 g of the soxhlet gangue was weighed into a 500 ml Teflon jar. 50 g of deionized water was added, and the combination was mixed on a rotary mixer for 10 mins at 60 rpm. The mixture was then transferred onto a 45 μm aperture sieve and vibrated for 5mins. After this, the solid on the sieve was spread out, and another 50 g of water was added to the solids followed by vibration for 5mins. This process was repeated until the liquid draining from the sieve was clear. About 15-25 repetition of 50 g water addition and sieving was required depending on the grade of the oil sand ore. The liquid collected from rinsing the sieve placed in an oven at 70°C to evaporate the water and collect the fine solids. The

coarse solids (≥45μm) were also dried at the same temperature. Dry sieving of the coarse solids using a 300 μm aperture 8" diameter sieve (ASTM E-11 Standard test sieve no. 50, Fisher Scientific Co., Waltham, MA) gave coarse solid of 45-300 μm.
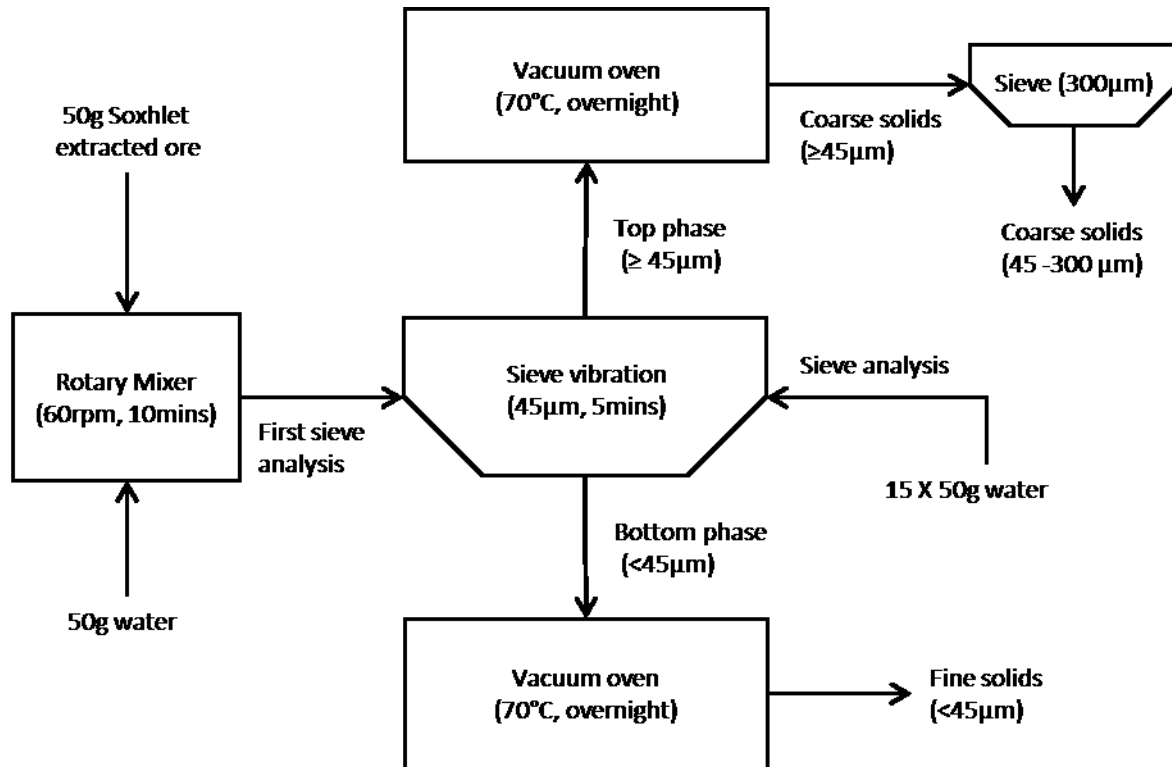
Figure 8: Protocol for extraction of fine solids

2.13 Particle size distribution Analysis

The particle size distribution of fines and coarse solid extracted from the dry soxhlet gangue were measured using a laser particle size analyzer (Mastersizer 3000, Malvern Instruments, Westborough, MA). The particle size distribution obtained was based on the volume fraction of the solids. Approximately 0.5g of solid was mixed with deionized water in a glass vial. The mixture was treated in an ultrasonic water bath for 15mins to break up aggregates and disperse the solids adequately. After initializing the analyzer and taking background measurements,

aliquots of sample were then transferred into the sample chamber of the analyzer until an obscuration of 5-10% was attained. An internal stirring device ensured that the particles stayed dispersed, while a laser beam illuminated the dispersed particles. A series of detector measured the intensity of light scattered by the particles for both red and blue light, and the mastersizer software analyzed the scattering data to calculate the particle size distribution [59].

2.14 Protocol for addition of fine solids

The protocol for the addition of fine solids during the preparation of reconstituted gangue with modified composition is shown in the flow sheet in Figure 9. First, the target ratio of fine solids in the reconstituted gangue was determined. Based on that, the required ratios by mass of fine solids to coarse solids are combined in a Teflon container. The mixture was mixed manually with a spatula for three mins and then put on a rotary mixer for further mixing at 20rpm for 1 min. It was then ready to be used as a dry soxhlet gangue in the reconstituted gangue protocol
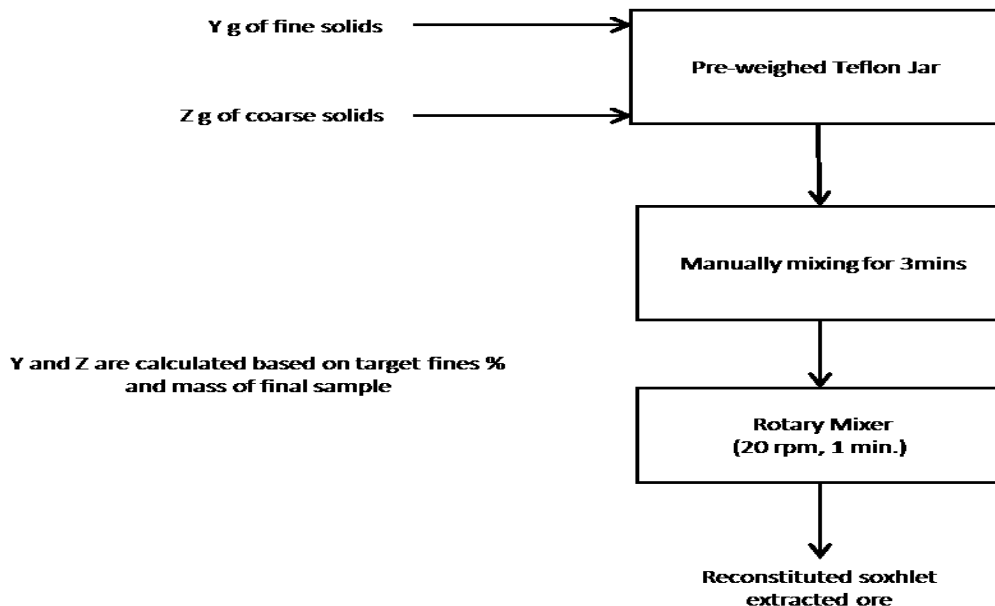
Figure 9: Protocol for addition of fines solids

2.15 Wettability of solids

The wettability of solids in oil sands is an important factor affecting the non-aqueous extraction of bitumen and the subsequent solvent recovery from the extracted gangue [60]. Particle partition, sessile drop contact angle, Washburn capillary rise and film flotation method have all been used for the determination of wettability of oil sands solids [34, 60, 61]. Particle partition method involves the introduction of the solid particles into a mixture of water and oil (or an immiscible hydrocarbon liquid) and measuring the distribution of the solids in the two layers after vigorous agitation. Although this method can successfully separate hydrophilic and hydrophobic particles, it is not sensitive enough to determine and distinguish the wettability of samples with small wettability differences [60]. As such, this method was not employed in our study.

2.15.1 Sessile drop contact angle

Static drop contact angle is one of the most common methods for determining the hydrophobicity of solids. It involves the measurement of a liquid (usually water) contact angle on the surface of solid or a compressed pellet of the solid. Often, a penetration time, which measures the time it takes for the water droplet to penetrate the pellet surface completely [34] is measured congruence with the contact angle.

A press (12 Ton E-Z Press^{TM}, International Crystal Laboratories, Garfield, NJ, USA) was used to make compressed pellet for contact angle measurement of fine solids. 0.1g of fine solids was pressed into a 1cm diameter pellet at a pressure of 4000psi. The compressed pellet was left overnight in an oven at 50°C to remove moisture from the surface before contact angle measurements. A Theta Optical Tensiometer (T200, Biolin Scientific, Stockholm, Sweden) was used to measure the contact angle. A deionized water droplet was carefully placed on the

compressed droplet (mounted on a stage) using a syringe equipped with an even tip needle. An image of the droplet was taken every 1s and processed to determine the static contact angle. Four-compressed pellets were prepared for each sample. Only one measurement was conducted per pellet, and the mean and standard deviation values were reported for the respective sample.

2.15.2 Film Flotation

Film flotation is a technique that assesses the wettability of particulate solids, in which hydrophobic and hydrophilic particles are partitioned by systematically varying the surface tension of the partitioning solution [62]. In film flotation, the particles placed on the liquid surface are imbibed into the liquid only when their critical surface tension is equal to or greater than the surface tension of the wetting liquid [63]. The procedure for film flotation used in this study is similar to that employed by Wang et al. [60]. Methanol-water solutions with a surface tension range of 22.5-72.0 mN/m were prepared by mixing methanol and deionized water at 0-100 volume % of methanol at 10% intervals. After mixing, each solution was placed in an ultrasonic water bath at 25°C for 15 mins to ensure homogeneity. Each solution was then transferred into separate 50ml glass bottle. Approximately 50 mg of fine solids were carefully sprinkled on the surface from a distance of about 2cm from the solution surface. A filter paper was to collect the particle floating after about 2 mins. The glass jars with sunk solids were dried and weighed to obtain the weights of the sunk solids. The filter papers used were left overnight in an oven at 80°C to remove moisture from the paper, and they were cooled and weighed before usage. The filter papers with floating solids were also dried and weighed for verification purposes. Figure 10 shows the apparatus for film flotation. In the picture on the left, the floating solids can be seen on the surface of the solution before they were separated out as shown in the picture on the right.

A frequency distribution from which the mean critical surface tension of the solids could be obtained by plotting the percent of floating particle as a function of the critical surface of the particle as determined by the surface tension of the solutions.

Figure 10: Film Flotation Apparatus

2.15.3 Washburn Capillary Rise

The wettability of coarse solids was determined using Washburn capillary rise method. This method utilized capillary pressure to drive liquid at an observable rate through a packed bed of solids in a vertical cylindrical tube [60]. The method required the preparation of identical beds of solid in the tube. The first bed was used to determine the capillary constant by carrying out measurement using a low surface tension and low viscosity fluid [64] (n-hexane was used for this purpose in our study). Once the capillary constant is determined, the contact angle could then be determined for the other packed bed for other liquids. 2.95g of coarse solids were weighed in a clean aluminum sorption tube lined with filter paper at the bottom. The tube was tapped gently to ensure a relative even bed surface, and then another filter paper was placed at the top of the solid. A Teflon-tipped plunger was inserted into the tube and hand tightened to compress the solids. The capped tube was then suspended in the tensiometer(Model K100, Krüss GmbH, Germany) above the liquid for contact angle measure. A mechanical control allows the

suspended tube to be brought close to the liquid surface. On activation in the software, an automated control brought the perforated base of the sorption tube in contact with the surface of the liquid at which point measurement are taking.

3 Results and Discussions

3.1 Properties of the Oil Sands Ore

The initial content of bitumen, water, and solids present in the rich-grade and low-grade oil sands ore, as determined by Dean-Stark extraction are given in Table 1. The table also gives the fine solids content of the ores as obtained by fine analysis. The balance of mass for the ore were coarse solids (particles larger than 45µm), and which are predominantly sand particles.

Table 1: Composition of oil sands ore

Component	Rich-grade	Low-Grade
Bitumen (wt. %)	13.5 ± 1.1	6.8 ± 0.5
Water (wt.%)	3.0 ± 0.9	9.5 ± 0.3
Fine solids (wt. %)	10 (n=2)	20 (n=2)

n = 2 indicate the result was obtained from duplicate analysis. n= 6 for other results

3.2 Recovery and Quality of the product bitumen

Non-aqueous extraction of low-grade ore with cyclohexane yielded a bitumen recovery of 63.2 ± 1.9 % compared to the 94.4 ± 1.7% obtained for the rich-grade ore by Nikakhtari et al. [26]. One potential explanation for the lower recovery in the low-grade (high fines) ore is that some bitumen were trapped in clays aggregates and thus, were not exposed to enough solvent during the extraction [8].

Analysis of the water content of the first supernatant and the combined second and third supernatants yielded 0.03±0.01 mg/g and 0.07±0.01 mg/g. These translates to about 0.01 wt % of water in the bitumen product. From mass balance calculation, this implies that less than 0.3 wt %

of the total water (present in the ore) migrates into the bitumen product. Thus, almost all the water originally present in the ore were retained in the extraction gangue.

The mass of fine solids released into the supernatants was negligible for low-grade ore. Less than 0.01g of fines was transferred into the bitumen product per 150g of low-grade oil sands extracted. Hence, just as with water, most of the fines in the low-grade and rich-grade ores remained in the extraction gangue. It is worth mentioning that a higher fraction (7-8%) of the fines present from rich-grade ore migrated into the product bitumen compared to low-grade ore. However, this fraction was less than 1% of the total oil sand mass used for the extraction. Nikakhtari et al. asserted that particle size of fine solids does not significantly influence their migration into the product bitumen [35]. One the other hand, the wettability of the solids was found to play a major role in the fine solids migration into the hydrophobic bitumen product. The higher migration of fine solids in rich-grade ore thus suggests the presence of more hydrophobic fines in rich-grade ore compared to low-grade ore. Nikakhtari et al. also showed a correlation between the water content of the ore and the amount of fine solids migrating into the product bitumen. Much more fines migrated into the bitumen product when water contents were below 3.4 wt % and above 13.4 wt % [35]. Connate water is believed to play an important role in binding up the fine solids and keeping them in the gangue [35].

3.3   Drying Curve Analysis

The changes in weight of the gangue sample over the duration of the dry experiment were recorded automatically and used to calculate the cumulative weight loss of the sample at different times in the experiment. A plot of the cumulative weight loss vs. plotted on the y-axis vs. cumulative time on the x-axis gave the drying curve for the samples. The early stages of drying exhibited maximum evaporation rates. All drying curves displayed an initial fast drying

period and end with very slow drying period, as seen in Figure 11. Solvent evaporation governed the initial drying period, while water evaporation dominated the slow drying stage [26, 33]. Using the same terminologies as employed by Siddhant et al. [31] for analyzing and comparing drying curves, we introduce the following factors
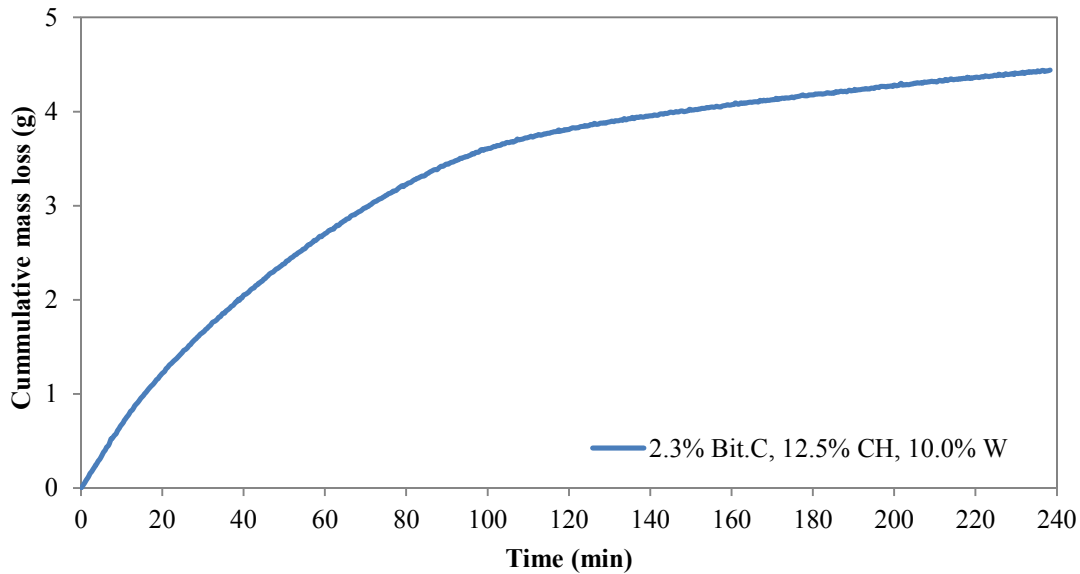
Figure 11: Mass loss curve for Low-grade extracted gangue. CH represents cyclohexane and W represents water. All % values are in terms of weight. The water content is on solvent-free basis

3.3.1 Initial Flux

The initial flux is the average evaporation flux taken over the first 10mins of drying. It is obtained from a linear regression plot and had a minimum coefficient of determination (R^2) of 0.99 for all samples. The initial flux was calculated by dividing the slope of the drying curve during the first 10mins of drying (Figure 12) by the surface area of the petri dish through which mass flux occurs. The equation for the calculating initial flux is given by the equation below

$$initial\ Flux = \frac{slope\ of\ the\ drying\ curve\ (first\ 10mins)}{Top\ Area\ of\ petridish\ (\Pi * r^2)} \qquad Equation\ 6$$

$y = 0.0683x - 0.0039$
$R^2 = 0.9993$

2.3% Bit.C, 12.5% CH, 10.0% W
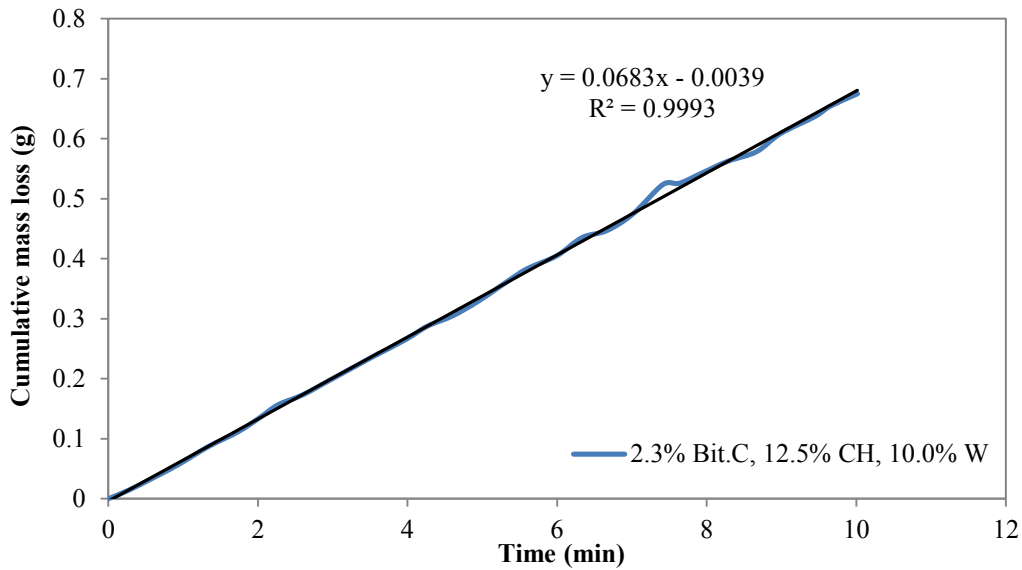
Figure 12: Linear regression plot for calculating average initial flux

3.3.2   Transition time:

The transition time or breakpoint refers to the point on the drying curve at which there is a dramatic change in the slope of the graph. It is the time at which the drying process moves from cyclohexane dominated evaporation to water dominated evaporation. The breakpoint was determined statistically using piecewise regression analysis over the transition region [31]. Piecewise linear regression comprises of two linear straight lines and is appropriate for scenarios where a single linear or non-linear regression model is unsuitable [65]. Siddhant et al. developed the piecewise regression model employed in this research work, using the function *nlinfit* (a non-linear iterative least square regression) in MATLAB 2015a over the transition time interval [31].

42

A 95% confidence interval for the transition time was obtained by bootstrapping, which involved the creation of random new data set from existing sample data set. Details of this statistical approach and corresponding MATLAB script for the model can be found in the Appendix section of Siddhant et al. [31]. Figure 13 shows excerpts from the MATLAB function showing the application of both linear regression model and the breakpoint or piecewise regression model. From Figure 13, it is apparent that the linear model does not work for estimating the transition time.
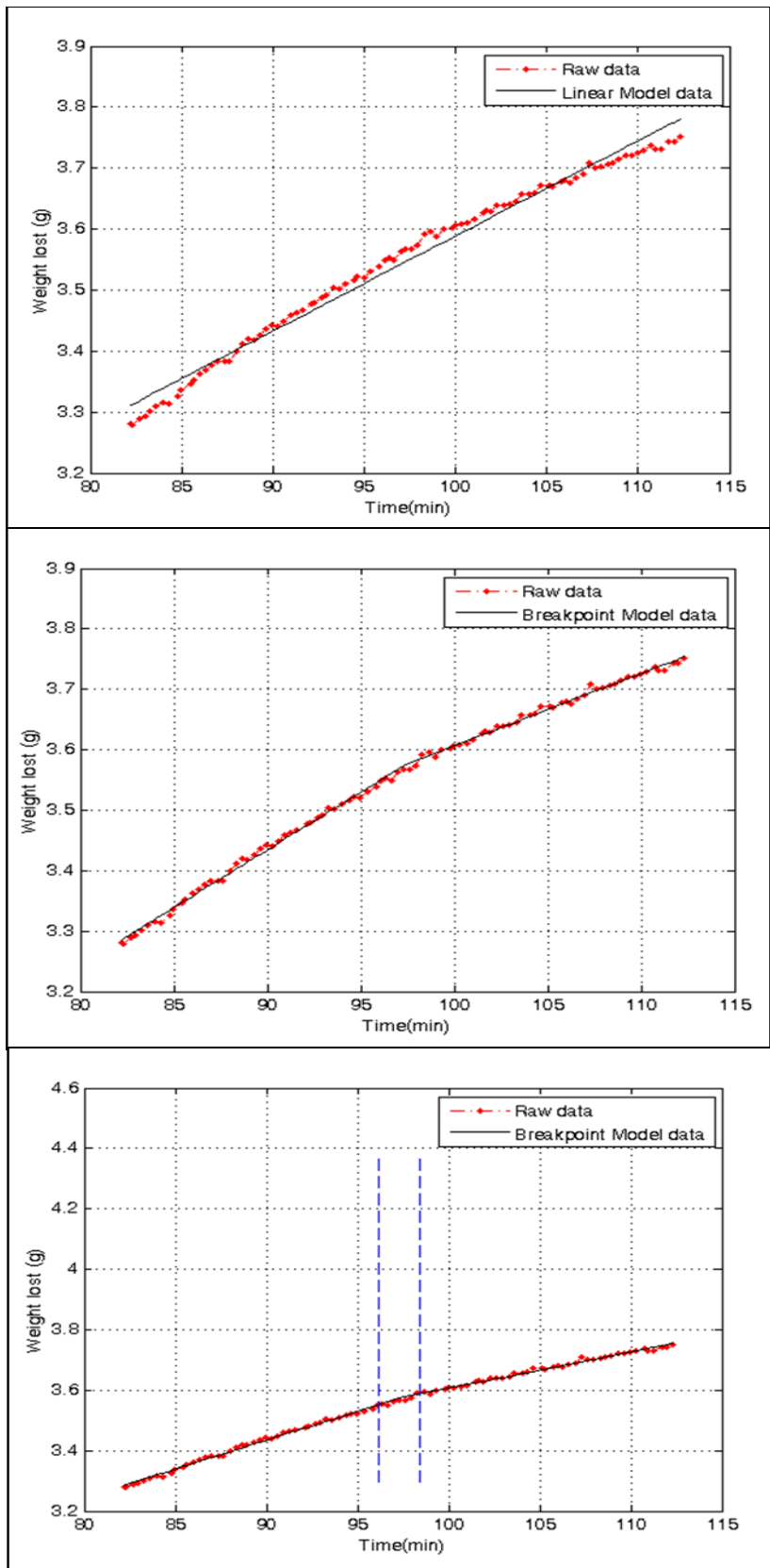
A: Linear regression model applied at the transition time interval

B: Breakpoint model (Piecewise regression) applied at the transition time interval

C: Transition time estimate using breakpoint model. The blue lines represent the 95% confidence interval for the transition time estimate

Figure 13: Linear regression vs. Breakpoint (Piecewise regression) model

3.3.3 Final Flux

The final flux is the average drying flux after the transition time interval. Just like the average initial flux, it is obtained from a linear regression plot, with a coefficient of determination of about 0.99. In the similar fashion, the final flux is calculated by dividing the slope of the drying curve after the transition time interval (shown in Figure 14) by the surface area of the petri dish through which mass flux occurs. It is represented by the equation 7

$$Final\ Flux = \frac{slope\ of\ the\ drying\ curve\ after\ transition\ time\ interval}{Top\ Area\ of\ petridish\ (\Pi * r^2)} \qquad Equation\ 7$$
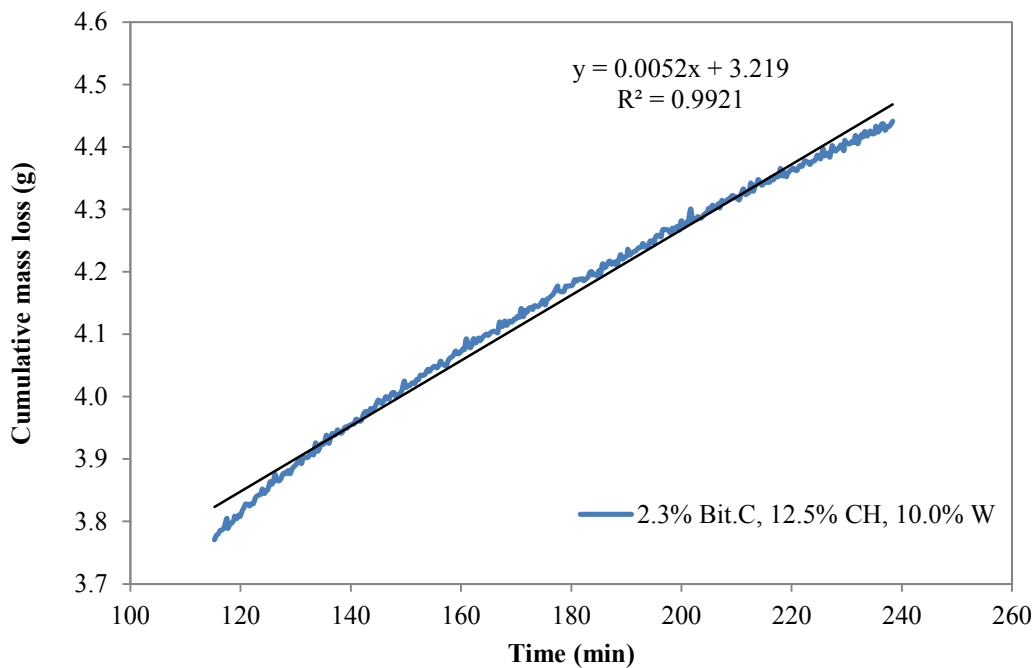
Figure 14: Linear regression plot for calculating average final flux

3.4 Drying Curve for the extracted Gangue

The drying curves for rich-grade extracted gangue have been demonstrated in the past in literature from Nikakhtari et al. [26, 33] and Siddhant et al. [31]. Nikakhtari et al. presented the drying curve in terms of the dimensionless weight loss of the tailings on the y-axis [26, 33]. The drying curves displayed the typical fast and linear initially mass loss followed by the slow and linear second stage mass loss. They demonstrated that the first stage was controlled by cyclohexane evaporation while water evaporation dominated the second slow stage. They also estimated the water content of the drying gangue sample by extrapolating the data for water evaporation. This method assumed no interaction between the cyclohexane and water during evaporation and yielded results that were consistent with initial water contents of the ore. Siddhant et al. successfully applied this method in their estimation of the water content of the rich-grade extracted gangue [21].

The drying curves for two low-grade extracted gangues are displayed in Figure 15 as a plot of the cumulative mass loss vs. time of drying. Similar to drying of rich-grade gangue, the curves showed a fast drying first stage and a slow drying second stage. In the same manner, the fast stage is controlled by solvent evaporation while the evaporation of water governed the slow stage. Preliminary drying experiments revealed that the low-grade extracted gangues took approximately 6hrs for complete drying i.e. to remove all solvent and water. This drying time was very high compared to the two-hour drying time required for rich-grade gangue in Nikakhtari et al. [26,33] and Siddhant et al. [31]. We attributed this longer time to be due to the significantly higher water content of the low-grade ore, and consequent gangue. As revealed by Dean-stark experiment, the low-grade ore contained about 10% water, compared to approximately 3% water content of the rich-grade ore. All this water remained in the gangue as

46

confirmed by Dean-stark extraction of the gangue and Karl Fisher titration of the product bitumen. This larger amount of the less volatile water contributed significantly to the longer drying time for the low-grade gangue. There was also the issue of higher residual bitumen content of low-grade gangue compared to most rich-grade gangue. This higher bitumen content, arising from the lower bitumen recovery, also contributed to the slow drying rate due to bitumen migration and plugging of pores [31].

Since our study was primarily concerned with solvent evaporation, the experimental drying time was reduced from 6hrs to an amount of time that was sufficient to evaporate the bulk of the solvent content of the gangue. Based on this, a drying time of approximately 4 hours (240mins) was chosen for the low-grade extracted gangues, as shown in Figure 15.
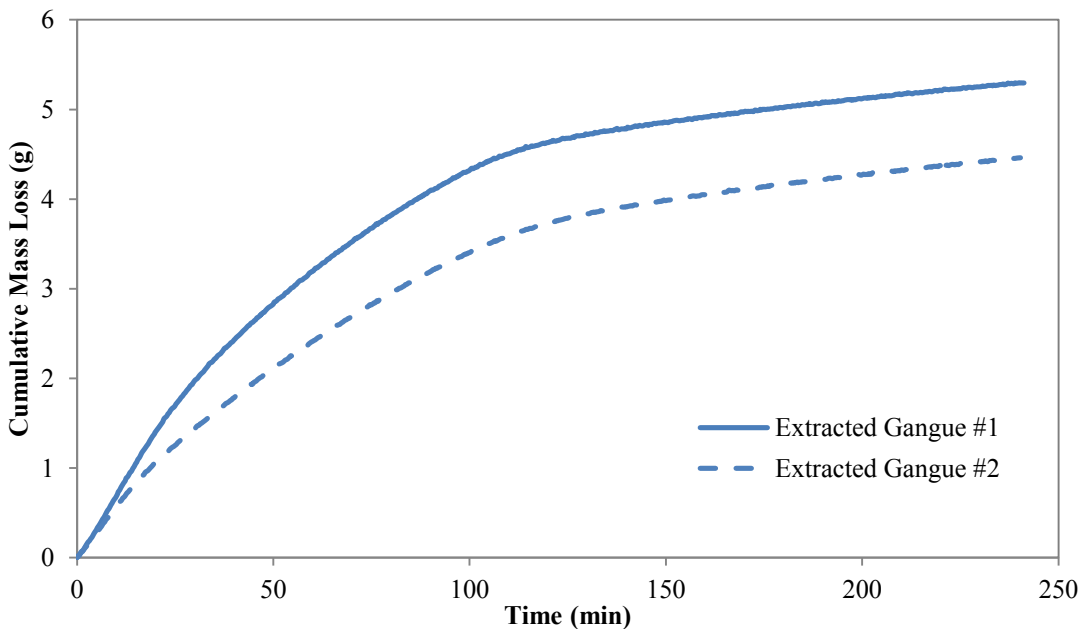
Figure 15: Drying curve for Low-grade extracted ore
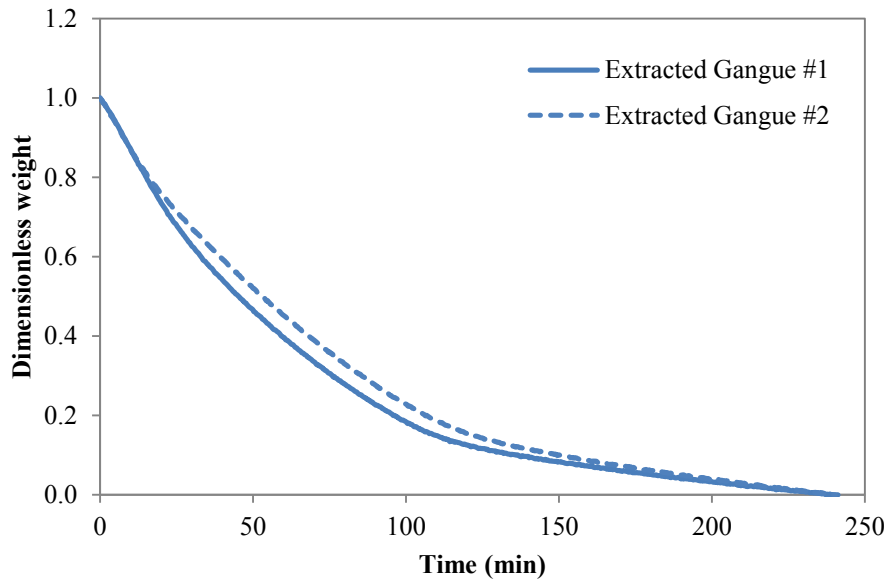
Figure 16: Dimensionless weight loss curve for Low-grade extracted gangue

Figure 16 is a representation of the drying curve in terms of a dimensionless weight loss of the gangue. The dimensionless weight was obtained by dividing the difference between the mass of the sample at any time during drying (M_s) and the initial mass of the sample(M_{si}), by the difference between the initial mass and final mass(M_{sf}) of the sample, as shown in the equation below

$$Weight\ loss\ = \frac{M_s - M_{sf}}{M_{si} - M_{sf}}$$ Equation 8

Unlike the rich-grade gangue samples, however, extrapolation of the water drying data did not provide a good estimate of the water content of the gangue. As stated earlier, the estimation of water content by extrapolation worked on the assumption that there is no interaction between cyclohexane and water during evaporation. This assumption appears to be valid at low water

48

content (such as at the 3.0 wt % of the rich-grade) relative to cyclohexane content of the drying sample. At such low level, the evaporation rate of water is (an order of magnitude) significantly lower than that of the cyclohexane which is present at a higher content in the gangue. However, at much higher gangue water content such as in low-grade ore, more water evaporates during the initial cyclohexane evaporation stage, making extrapolation and the assumption of no interaction less accurate. However, although the water evaporation was higher for the low-grade sample with 10 wt % water, the low volatility of water means that the water evaporation was still very low in comparison with the cyclohexane evaporation, making the statement of cyclohexane dominated initial drying stage still accurate.

Thus, the compositions of the extracted gangues were determined by Dean-stark analysis. Approximately 40g samples of frozen extracted gangue were used to this analysis. Frozen samples were used to reduce solvent loss during preparation. The ratio of Soxhlet sand to water in the gangue was examined, and it corresponded to the ratios present in the original ore. This observation supported the assertion that water is retained in the gangue as previously indicated by the insignificant water content of the bitumen product.

CHNS analysis determined the bitumen content of the low-grade gangue. In general, low-grade extracted gangue had a composition range of 11-15% cyclohexane, with a mean concentration of 12.8% and a standard deviation of 1.0%; an average water content of $9.9 \pm 0.2\%$ on a cyclohexane free weight basis and a bitumen carbon content of $2.2 \pm 0.2\%$. The composition of the extracted gangue #1 and #2 are listed Table 2.

Table 2: Composition of Low-grade extracted gangue.

Fluid component (wt)	Bit.C (%)	Cyclohexane (%)	Water (%*)
Extracted Gangue #1	2.1	13.0-13.5	10
Extracted Gangue #2	2.0	12.0-12.5	10

*Water content is on a solvent-free weight basis

Reconstituted gangues of similar composition as the extracted gangue #1 and #2 were prepared for the low-grade sample. The two reconstituted gangues prepared had a bitumen carbon content of $1.9 \pm 0.1\%$, cyclohexane content of 13-14% and 10% water content on a cyclohexane free weight basis. Figure 17 shows the drying curve for reconstituted gangue #1 and #2.
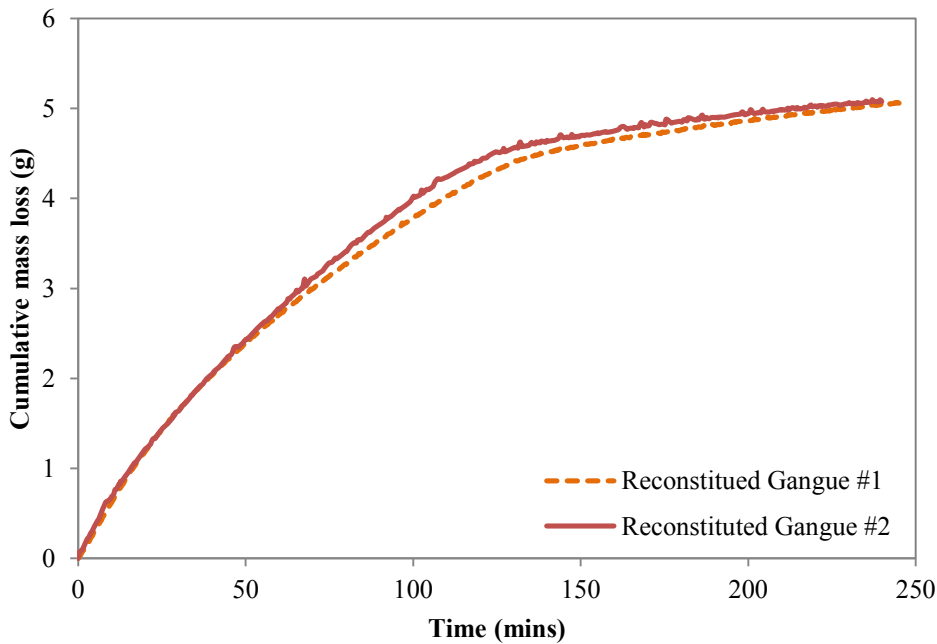
Figure 17: Drying curve for Low-grade reconstituted gangue

3.5 Comparison of drying curves extracted gangue and reconstituted gangue

Comparison of drying curve for rich-grade extracted gangue and reconstituted gangue can be found in Siddhant et al. [21].

Drying experiment for the extracted and reconstituted low-grade gangues were conducted under similar drying conditions of air flow, temperature, and relatively constant humidity. A comparison of the drying curves is shown in Figure 18.
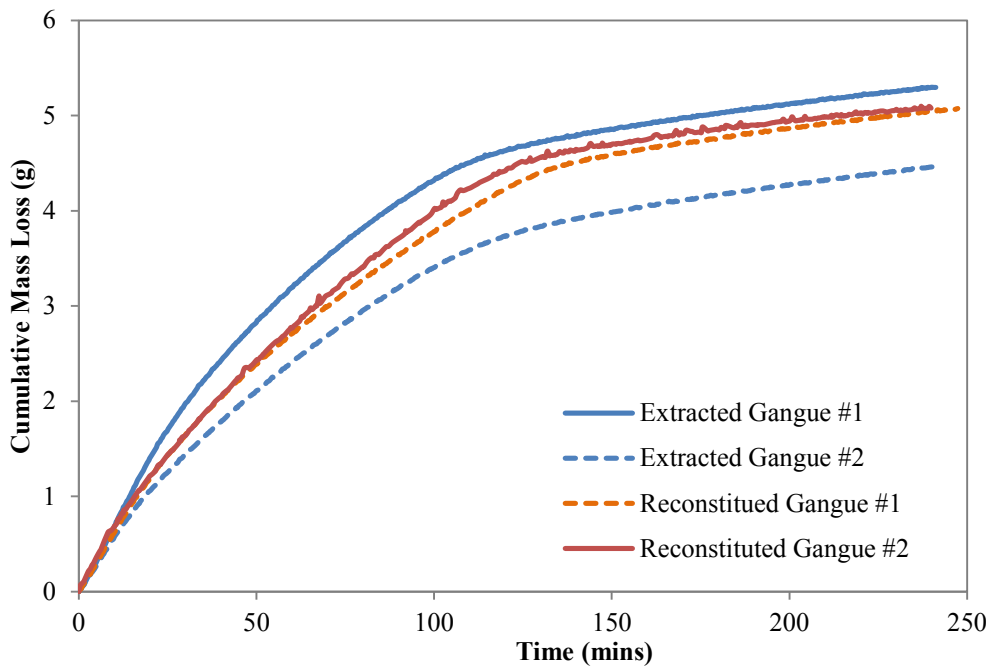
Figure 18: Drying curve comparison of Low-grade extracted and reconstituted gangue

Each drying curves was also evaluated using the different elements of the drying curve discussed earlier, namely the initial flux, the transition range and the final flux. The results of this evaluation are presented in Table 3 below

Table 3: Comparison of initial flux, Transition time interval and Final flux of Low-grade extracted and reconstituted gangue

Sample	Initial flux g/(cm^2.min)	Transition time interval (mins)	Final Flux g/(cm^2.min)
Extracted Gangue #1	3.53 e -03	106 - 109	2.65 e -04
Extracted Gangue #2	2.94 e -03	117 - 120	2.55 e -04
Reconstituted Gangue #1	3.22 e -03	130 - 133	2.55 e -04
Reconstituted Gangue #2	3.50 e -03	123 - 126	2.44 e -04

It can be seen from the Table 3 that the initial flux for the extracted gangue and the reconstituted gangue are similar, and the samples had the same order of magnitude. The transition time intervals for the reconstituted gangues were slightly higher than those for the extracted gangues. However, they fell within a 10% relative margin of error for the upper limit of transition time interval of the extraction gangue. The final flux values of the extracted and reconstituted gangues are identical, and they all are an order of magnitude lower that initial flux. Recall that final flux corresponds to the evaporation of water from the gangue.

Furthermore, there are other factors worth considering when comparing the extracted and reconstituted gangues. These factors are related to the bitumen migration. As stated earlier, migration of residual bitumen has been observed during the drying of packed beds of rich-grade extracted gangue [17, 21]. Bitumen migration was also observed in our experiments for both the low-grade extracted gangue and reconstituted gangue, confirming at the very basis that the primary drying mechanism and transport phenomena are the same. Figure 19 shows the frame

shot of the top and bottom layer of reconstituted gangue which depict the bitumen migration. Notice the dark bitumen-enriched top layer compared to the bottom layer
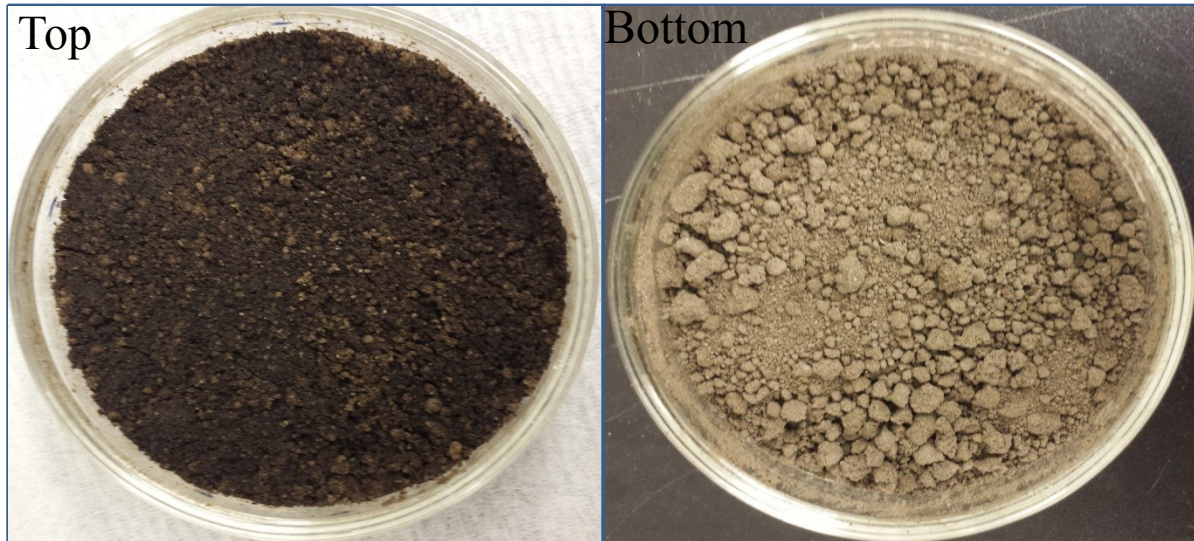
Figure 19: Top and bottom layer of Low-grade reconstituted gangue

Also, lumps formed during the drying of reconstituted low-grade gangues, as is visible in the bottom layer in Figure 21, which also occurred in the extracted low-grade gangue.No such lumps were observed during the drying of rich-grade extracted or reconstituted gangues. The lumps could be attributed to the higher water content of the low-grade gangues that led to stronger binding of fines and solids together.

Carbon content obtained from CHNS analysis of the gangues before drying, and of the top and bottom layer of the gangue after drying were used to assess the migration of bitumen. Given

x_s = toluene insoluble carbon % of the gangue obtained from CHNS analysis of the bitumen-free soxhlet gangue

x_i = initial carbon % of the extracted or reconstituted gangue

x_{TL} = carbon % of the top layer after drying experiment

x_{BL} = carbon % of the bottom layer after drying experiment,

we obtain

i)   The initial bitumen associated carbon content of the gangue as

$$initial\ Bit.C\ \% = x_i - x_s \qquad\qquad Equation\ 9$$

ii)   Bitumen carbon content of the top layer as

$$Top\ layer\ Bit.C\ \% = x_{TL} - x_s \qquad\qquad Equation\ 10$$

iii)   Bitumen carbon content of the bottom layer as

$$Bottom\ layer\ Bit.C\ \% = x_{TL} - x_s \qquad\qquad Equation\ 11$$

These calculations were based on the valid assumption that bitumen is the only other source of organic carbon in the extracted and reconstituted gangue. x_s was obtained after exhaustive toluene extraction. x_{tl} and x_{bl} are obtained after 4hrs drying experiment while x_i was before the experiment. All samples were dried in a vacuum oven at 70 °C for 24 hrs prior to CHNS analysis.

Based on the above, we define two further terms used for evaluating the extent of bitumen migration; namely, enrichment ratio and bitumen migration fraction.

3.5.1   Enrichment ratio

The enrichment ratio describes the enrichment of bitumen in the top layer of the drying gangue relative to the initial bitumen content of the gangue. It can be defined as the ratio of the bitumen carbon % of the top layer to the bitumen carbon % of the initial gangue sample, as shown in the equations below

$$Enrichment\ ratio = \frac{Top\ Layer\ Bit.C\ \%}{Initial\ Bit.C\%\ of\ gangue} \qquad\qquad Equation\ 12$$

$$= \frac{(x_{TL} - x_s)}{(x_i - x_s)} \qquad\qquad Equation\ 13$$

3.5.2 Bitumen Migration Fraction (BMF)

Bitumen migration fraction is a more comprehensive factor than the enrichment ratio as it accounts for the mass of the migrating bitumen. BMF is defined as the ratio of the mass of bitumen migrating into the top layer to the total mass of bitumen present in the gangue. The formula for calculating BMF incorporates the masses of the top and bottom layers, as well as the enrichment ratio.

$$Bitumen\ Migration\ Fraction = \frac{(M_{bitTL})_f - (M_{bitTL})_i}{(M_{bitTL})_i + (M_{bitBL})_i} \qquad\qquad Equation\ 14$$

$$= \frac{(x_{TL} - x_s)}{(x_i - x_s)} * \frac{y_{TL}}{y_{TL} + y_{BL}} \qquad\qquad Equation\ 15$$

where $(M_{bitTL})_f$ and $(M_{bitTL})_i$ are the final and initial mass of bitumen in the top layer respectively. $(M_{bitBL})_i$ is the initial mass of bitumen in the bottom layer. y_{TL} and y_{BL} are the masses of the dried top and bottom layer respectively.

Note that there is a maximum error of about 2.4% associated with the BMF calculation for an approximate 2% bitumen carbon content of extracted and reconstituted gangue [31]. This error originates from the fact that mass fraction of carbon in bitumen is 0.833, and so, 1% Bit. C is equivalent to 1.2% bitumen. This scaling factor was not carried through in the BMF calculation and account for the insignificant 2.4% error in the bitumen mass calculation for 2% Bit. C.

Details of the calculation and propagation of this error are outlined in Appendix of Siddhant et al. [31].

The enrichment ratio and bitumen migration fraction for the extracted and reconstituted gangues #1 and #2 are shown in Table 4

Table 4: Comparison of enrichment ratio and bitumen migration fraction for Low-grade extracted and reconstituted gangue

Sample	Enrichment ratio	Bitumen Migration Fraction
Extracted Gangue #1	1.93	0.38
Extracted Gangue #2	1.66	0.28
Reconstituted Gangue #1	1.75	0.21
Reconstituted Gangue #2	2.02	0.29

As shown by the Table 4, the enrichment ratio and bitumen migration fraction of the extracted and reconstituted gangues overlap and are in accord. Given the agreement in these values as well as in the initial flux, transition time interval and final flux mentioned earlier, it is sufficient to conclude that the behavior of the low-grade extracted and reconstituted gangue are similar, and the drying mechanism is consistent in both. On this basis, the rest of the experiments in this research were conducted using reconstituted gangue due to the advantage of customizing its composition to enable the study of the effect of gangue component on solvent recovery.

3.6   Effect of Fines solids in Solvent Recovery

The composition of fine solids in oil sands varies with the source and quality of the oil sands. Dean-Stark extraction followed by fine solids analysis revealed that the two grades of oil sands used in our experiment had very different fine solids content. Rich-grade ore had approximately 10% fines content while Low-grade ore had about 20% fines content. We have also seen that essentially all of the fine solids are retained in the gangue after extraction. As a preliminary approach to investigating the effect of fine solids on solvent recovery, we prepared reconstituted gangue of rich-grade and low-grade oil sands of similar composition of fluids (solvent and water). The role of bitumen in reducing solvent recovery in the gangue has already been studied extensively by Siddhant et al. [31] and it was confirmed in our preliminary study. The focus of this paper was to elucidate the role of fine solids on solvent recovery from reconstituted gangue. As such, bitumen was excluded from the following experiments. We present and compare reconstituted gangue with the unchanged original fines composition of rich-grade and low-grade gangue, fixed cyclohexane and water contents of 12 % and 3.7 %* (solvent free basis) respectively, and no bitumen. The reconstituted gangue will hereafter be referred to as re-gangue.

First, let us examine the evaporation of solvent from rich-grade re-gangue containing only 12% cyclohexane as shown in Figure 20
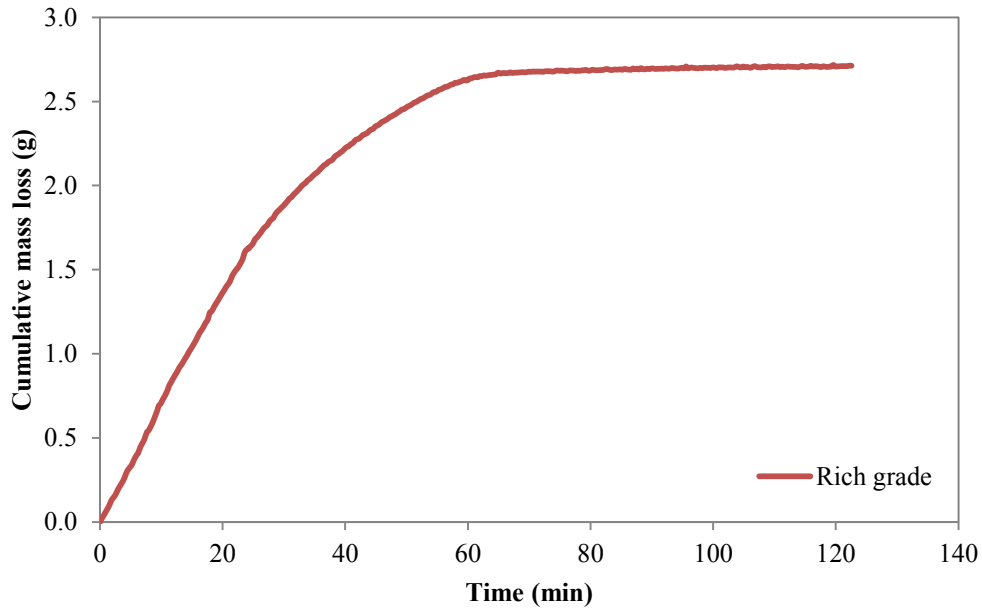
Figure 20: Drying curve for Rich-grade re-gangue containing 12% cyclohexane

Recall that the presence of liquid films accelerates the drying of porous media. Liquid films are present in the stage 1 evaporation of the fluid, and they maintain capillary connectivity to the surface. Figure 21 depicts the drying kinetics for cyclohexane evaporating from the gangue bed. Stage 1 is fast, constant rate period that is governed by external mass transfer at the surface, while stage 2 is slow rate period governed by vapor diffusion within the media.
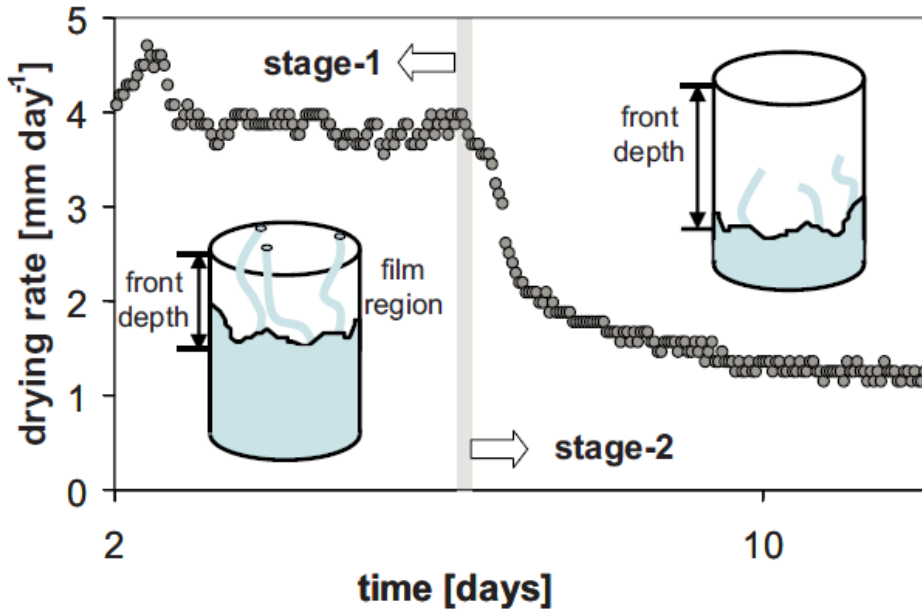
Figure 21: Stages of drying in porous media (Lehman et al., 2008)
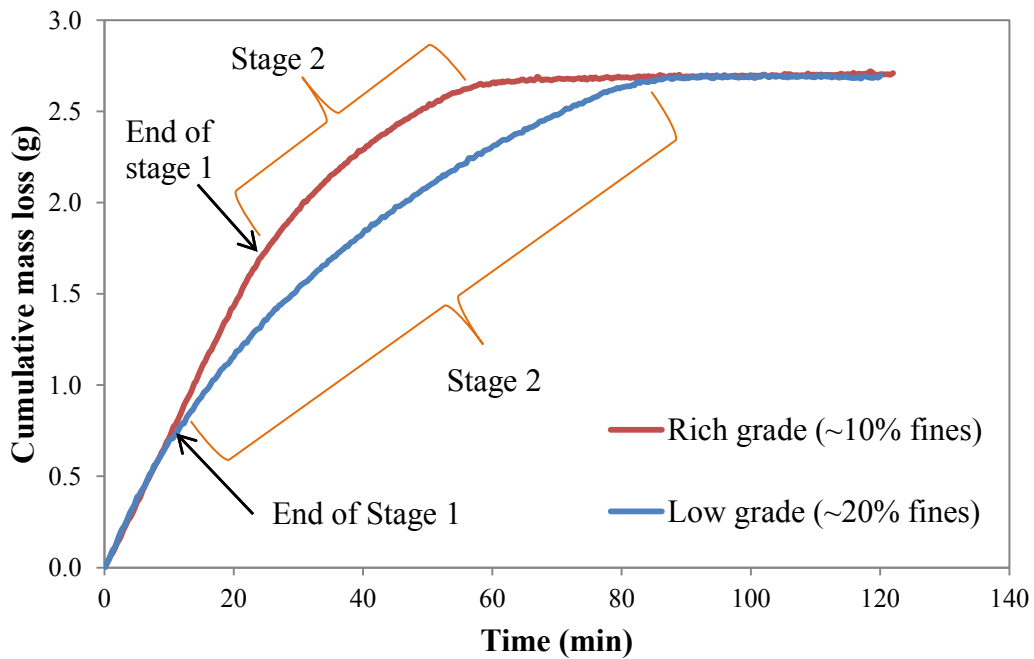
Figure 22: Drying Curve for Rich vs. Low-grade re-gangue containing 12% CH

Table 5: Initial flux and residual cyclohexane content of Rich and Low-grade re-gangue containing only 12% CH

Sample	Initial Flux $g/(cm^2.min)$	Residual cyclohexane (ppm)
Rich-grade re-gangue	3.9 ± 0.4 e -03	0.2 - 4.0
Low-grade re-gangue	4.0 ± 0.1 e -03	49.1 - 54.0

Figure 22 and Table 5 compare the drying curve and results for rich-grade and low-grade re-gangue containing 12% cyclohexane. It can be seen from the graph and table that the initial cyclohexane evaporation flux is the same in both the rich-grade and low-grade re-gangue. Low-grade re-gangue with higher fine solids content had a higher residual solvent content than the rich-grade equivalent. It is also evident from the graph that a longer time was required to reach the plateau in the curve for the low-grade sample than for rich-grade sample. The plateau which occurred at about 50mins for rich-grade sample and 80mins for the low-grade sample corresponds to the time at which most of the cyclohexane has been removed from the gangue. The time difference implies that given the similar initial cyclohexane content of both samples, the solvent removal process was slower in the low-grade sample. On further inspection of the drying curves, we also see that duration of the constant rate period (CRP) or stage 1-evaporation was longer for rich-grade sample (~20mins) than for low-grade sample (~9mins). The longer duration of the fast stage 1 evaporation solvent from rich-grade re-gangue was responsible for the shorter length of time to remove most of its solvent. On the other hand, for low-grade gangue with a shorter duration of Stage 1 solvent evaporation, a larger proportion of the evaporating

solvent had to be removed through the much slower vapor diffusion process of the falling rate period (FRP) or Stage-2 evaporation.

When we consider the drying curve for rich-grade re-gangue containing both cyclohexane and water, we observed a typical drying curve for both extracted and reconstituted, rich-grade or low-grade gangue containing both fluids (in the presence or absence of bitumen). Figure 23 show the important regions of consideration for the drying curve.
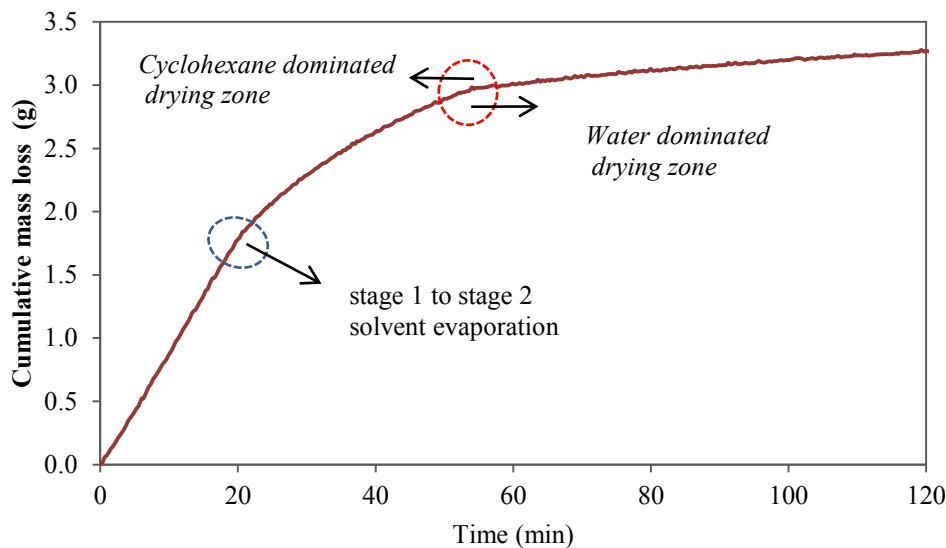
Figure 23: Typical drying curve for both extracted and reconstituted gangue

In Figure 23, the inflection point in the blue circle represents the point of transition from the fast rate stage-1 solvent evaporation to the slower stage-2 evaporation. This point was present in the drying curve for samples containing the solvent only. However, unlike samples containing only cyclohexane in which a plateau marked the end of evaporation of the bulk of the solvent, the sample containing both cyclohexane and water exhibited a shallow slope that corresponded to the evaporation of water. The inflection point at this region, circled in red in Figure 23 refers to

the transition from the solvent-dominated to the water-dominated period of drying. Earlier, we referred to this region over which the transition occurred as the transition time interval. Note that a small fraction of water evaporates during the solvent evaporation stages, but it is insignificant compared the amount or rate of solvent evaporation.

Let us now compare the drying curves for rich-grade and low-grade re-gangue containing 12% CH and 3.7%* W.
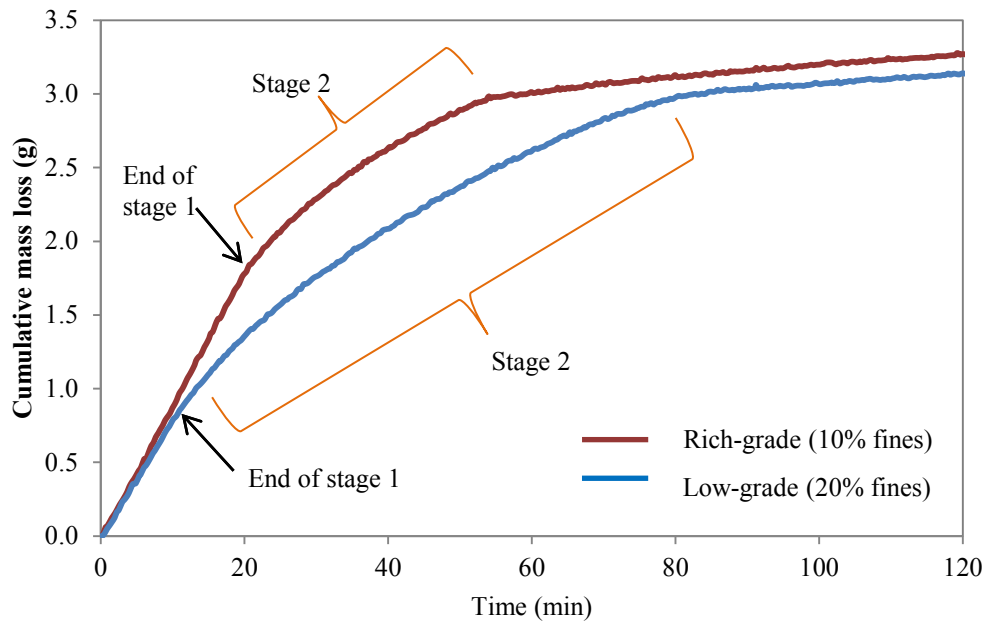
Figure 24: Drying curve comparison for Rich-grade vs. Low-grade re-gangue containing 12% CH and 3.7 %* W

Table 6: Initial flux and residual cyclohexane content of Rich-grade and Low-grade re-gangue 12% CH and 3.7 %* W

Sample	Initial Flux	Transition time	Residual

	g/(cm^2.min)	(min)	cyclohexane (ppm)
Rich-grade re-gangue	4.4 ± 0.1 e -03	52-56	22 - 29
Low-grade re-gangue	4.3 ± 0.2 e -03	77-83	23 - 37

Figure 24 shows a distinct difference between drying curve for both rich-grade and low-grade gangue containing cyclohexane and water. Much like the curves for samples containing 12% CH only in Figure 23, rich-grade samples in this case also exhibited a longer duration of the fast stage 1 evaporation and shorter duration of the slow stage 2 cyclohexane evaporation. Conversely, low-grade had a shorter stage 1 and longer stage-2 cyclohexane evaporation. Due to the slower drying process for cyclohexane in the low-grade sample, the transition to the water-dominated drying stage occurred at a much later time compared to rich-grade sample. This transition for low-grade gangue occurred over 20mins later than that for rich-grade as shown in Table 6.

An interesting initial observation we made was that there was no significant difference in the residual cyclohexane content for rich-grade and low-grade samples in the presence of water. The role of water in solvent recovery was not addressed in this research, but it is an interesting subject for our future study. Water evaporation is known to be affected by the relative humidity of the drying environment [33]. When the rich-grade and low-grade samples were dried on the same relative humidity condition, the same final flux of 2.1 e – 03 g/(cm^2.min) and a more differentiated residual cyclohexane content was obtained for rich-grade sample (29ppm) and low-grade sample (37ppm) of similar initial composition.

Due to the difference that can arise from variation in relative humidity, temperature, and air flow rate, it was important that samples to be compared be dried under similar controlled conditions. Consequently, measures such as performing same-day drying experiments for samples for comparison were taken, thereby minimizing fluctuations in relative atmospheric humidity and air flow

So far, we have seen from the fine solids analysis that rich-grade and low-grade ore have approximately 10% and 20% fine solids respectively. We also know from centrifugation of bitumen product that the bulk of the fines end up in the gangues, at such the gangue has similar fine content as the initial ore. By comparing the drying curve of rich-grade and low-grade re-gangue of same liquid composition, we observe that overall rate of solvent removal is slower for low-grade samples which contain higher fines content than rich-grade samples. This observation suggests that an increase in fine solids content of the gangue leads to a decrease in solvent recovery rate. The question that arises then is how an increase in fine solids content exacts its influence on solvent recovery? To answer this, we considered the major changes that occur in the gangue as the fine solids content increases.

Fine solids in oil sands are defined as particles below 44μm in size. Hence, increasing the fine solid content of a gangue changes the particle size distribution of the gangue. Also, fine solids in oil sands are known to have a range of surface properties, from hydrophobic to hydrophilic [35]. Fine solids isolated from oil sands after non-aqueous solvent extraction are also more hydrophilic than those from water-based extraction because of the much higher bitumen extraction efficiency of non-aqueous extraction [60]. The higher migration of fine solids into bitumen product during extraction of rich-grade ore compared to low-grade ore suggests that wettability difference exists between the fines of both ores. In fact, Nikakhtari et al. showed a

correlation between the fine solids content of oil sands ore and the hydrophilicity of the fine solids [35]. Results indicated an increase in the wettability of fine solids that corresponded with an increase in the fine solids content of the ore as depicted in Table 7.

Table 7: Contact angle of fine solids from Alberta oil sands (values obtained from Nikakhtari et al., 2014)

Fines content of ore (%)	8.6	15	18
Contact angle (°)	42	35	23

We did not find any data in open literature on the wettability of coarse solids from non-aqueous solvent extraction. However, comparison of wettability data for solids from the water-based extraction of rich-grade(good processing) and low-grade (poor processing) ores, showed that the fines solids are more hydrophilic than coarse solids [34]. We had no reason to expect a different trend for the solids obtained from non-aqueous extraction. On this basis, it is apparent that not only does particle size (pore size) distribution of the gangue change with increasing fine solids content, but the wettability of the pore also change. Prat (2006) confirmed that the contact angle and pore size greatly affect drying during the Stage 1 evaporation (CRP) where liquid films are important [38].

3.6.1   Effect of Particle Size Distribution (Pore size)

The demand for evaporation is supplied by capillary induced liquid flow from large pores at the drying front to supply water evaporating from small pores at the surface during stage-1 evaporation [66, 67]. The extent of the liquid film region which control the duration of stage 1

evaporation is determined by a balance between the flow inducing capillary forces and counteracting gravitational and viscous forces [49]. These forces are affected not only by the mean pore size distribution but also by the width of the pore size distribution [43, 49]. Stage 1 evaporation ends when resisting gravitational and viscous forces exceed the capillary forces [43]. To better understand the effect of the particle (pore) size distribution on the duration of stage 1 evaporation, we examine several examples of previous work.

Lehman et al. performed water drying experiments from two quartz sand porous media of different particle size distributions [49]. They used 'fine sand' and 'coarse sand' with particle sizes 100-500µm and 300-900 µm respectively. They presented their results on the duration of the stage 1 evaporation for these samples graphically. The result showed that the duration of initial high rate period of evaporation (i.e. stage 1 evaporation) in the fine sand was twice as long as in the coarse sand. Also, tw0 times as much water had evaporated for by the end of the stage 1 evaporation for fine sands than for coarse sand. These observations suggest that increasing the fine solids content in the sand sample would increase the duration of stage 1 evaporation.

Rad et al. studied the effect of pore size on salt precipitation during evaporation from porous media [67]. They performed drying experiments using six samples of quartz sands of differing particle size distribution and kept the average porosity of the media constant. Salt migration during the drying of salt-water solution from porous media is known to occur via similar thick liquid film flow as observed in the drying of water [67, 68]. Rad et al. observed that salt precipitation occurred at fine pores at the surface, which were the preferential site of water evaporation in porous media [67]. Large pores which are formed by larger particles are invaded

by air at early stages of drying while smaller pores remained saturated due to capillary effect [43, 67]. They also observed that at any time during the dying, the surface saturation of the media decreased as the particle size increased. They attributed this effect to the reduced hydraulic connectivity to the media surface, and it implied that drying front receded below the surface earlier. For such larger grain size sample, fewer fine pores at the surface resulted in a shorter stage 1 evaporation (and precipitation) [67]. In other words, the duration of stage 1 evaporation increases as particle or pore size decreases.

Yiotis et al. experimented with the drying of hexane and pentane from packed beds of hydrophobic glass beads [45]. Their experiment confirmed that capillary flow through liquid film also enhances the drying of these organic solvents. They found that the gravity effect dominates in large pore sizes leading to an earlier detachment of liquid film from the surface and shorter films. On the other hand, for small pore sizes, capillary force is stronger and results in longer films and longer stage-1 duration. Theoretical calculation corroborated the results of their experiment.

By these three works, it can be concluded that a decrease in the representative particle size distribution (pore size) of the gangue should result in an increase in the duration of stage 1 evaporation of the solvent. In more related terms, we would expect the low-grade (higher fines) samples to have longer stage 1 evaporation than the rich-grade (low fines) samples. However, this was not the case as observed. Let us now consider the effect of a change in wettability of the pore wall which arises from the presence of more hydrophilic fine solids.

3.6.2 Effect of Changes in wettability

Shokri et al. studied the evaporation of water from hydrophilic (HI) and hydrophobic (HO) quartz sand media [52]. The samples had the same particle size distribution (300-900) μm and were dried under the same condition of ambient temperature, relative humidity, bed depth and constant porosity. The water contact angles for the hydrophilic and hydrophobic sands were 0° and 88° respectively.
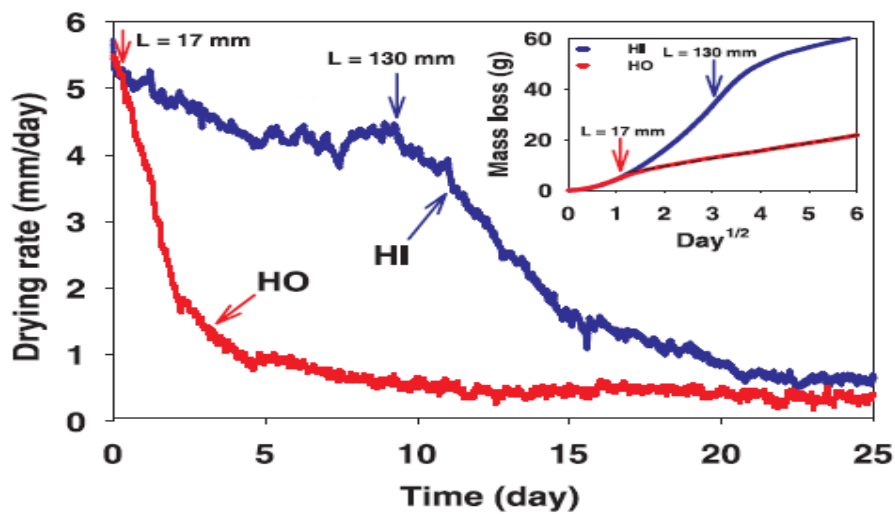
Figure 25: Drying curve for hydrophilic (HI) and hydrophobic (HO) porous media (Shokri et al., 2009)

Figure 25 shows that the characteristic length, L (the drying front depth at which the transition from stage 1 to stage 2 evaporation occurs) is significantly longer for hydrophilic sand (130mm) than for hydrophobic sand (17mm). Likewise, the duration of the stage 1 evaporation was longer for HI sand than for HO sand; this was evident by the longer period of surface saturation for HI sand [52]. Also, the duration of stage 1 evaporation was found to decrease as increasing fractions of HO sand were mixed with the HI sand. Also, they observed a drastic change in the

evaporation trend and duration of the stage 1 evaporation from the addition of 10% HO sand as shown in Figure 26.
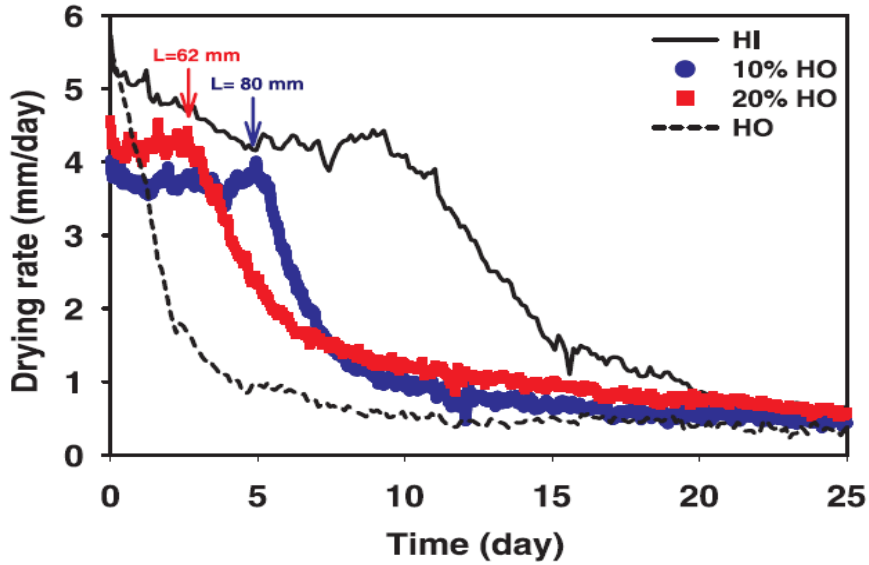

Figure 26: Drying curve for sands containing different fraction of hydrophobic grains (Shokri et. al., 2009)
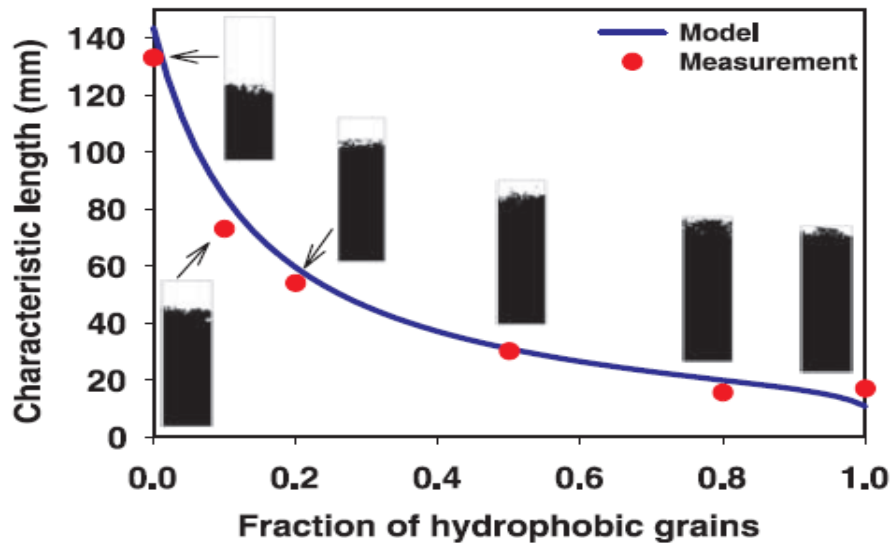
Figure 27: Characteristic length as a function of hydrophobic grain fraction (Shokri et al., 2009)

As shown in Figure 27, there is an exponential decrease in the characteristic length even with the addition of small amount of hydrophobic fractions. Shokri et al. showed that the introduction of hydrophobic particles to a mixture creates pore structure with weaker capillary forces [52, 53]. They concluded that diminishing capillary driving forces are the net effect on evaporation from mixed-wettability media. This observation is further supported by the work of Al-Futaisi et al. [69] and Wallace et al. [70] who showed capillary pressure could change significantly in response to a small change in contact angle in the pore. Wallace et al. concluded that contact angle plays a significant role in the drainage of wettable porous media [70].

With regards to the addition of hydrophilic particles and their effect on the evaporation of hydrophobic liquid like cyclohexane, the same effect of a reduction in capillary force with increasing hydrophilic particle fraction would be expected, just as observed with hydrophobic particles and hydrophilic water. Thus, on the basis of a higher content of hydrophilic fine solids, we expect low-grade (high fines) samples to have shorter stage 1 evaporation than rich-grade (low fines) samples. Considering the results obtained in comparison in Figures 22 and 24, and the associated tables 5 and 6, it appears that the effect of wettability change from the addition of fine solids dominates the effect of the change in particle size distribution resulting from the addition. To state explicitly, the loss in capillary pressure due to the presence of the more hydrophilic fine solids outweighs the gain in capillary pressure arising from the change in particle size distribution due to the fine solids.

3.6.3   Particle size distribution and Wettability of Solids

To verify our assertion, we proceeded to analyze each grade samples further and to perform more controlled experiment. We extracted fine solids from both rich-grade and low-grade soxhlet sand

and measured the particle size distribution and wettability for fines solid (<45µm) and coarse solids (45µm-300µm).

For particle size distribution, the D10, D50, and D90 of the fine solids and coarse solids for each sample grade are shown in Table 8

Table 8: Particle size distribution of fine solids and coarse solids of Rich-grade and Low-grade ore

Sample	Constituent solid	D10 (µm)	D50 (µm)	D90 (µm)
Rich-grade	Fine (-45µm)	1.6 ± 0.1	9.0 ± 0.9	41.3 ± 3.4
	Coarse(+45µm - 300µm)	122 ± 4	190 ±1	292 ± 4
Low-grade	Fine (-45µm)	1.6 ± 0.1	8.9 ± 1.2	38.5 ± 2.4
	Coarse(+45µm - 300µm)	75 ± 5	155 ± 5	277 ± 5

From Table 8, we see that there is no significant difference between the particle size distribution of the fine solids of low-grade and rich-grade samples. Hooshair et al. had a similar observation when analyzing high fines and low fines oil sands ore from Syncrude [73]. They found no significant difference in the morphology of clay particles from the two ore, with the particle size from the high fines (low-grade) ore being only slightly smaller. For the coarse solids, however, the D10 and D50 are significantly smaller for the low-grade sample than the rich-grade sample. This result indicates that the low-grade ore had a greater content of smaller sized solid particles compared to rich-grade ore.

Static sessile drop contact angle measurement coupled with penetration time gave the contact angle and penetration time of 1cm pellet as 51.3° and 39.0s for rich-grade fine solids and 42.4°and 15.0s for low-grade fine solids. Wang et al. recommended film flotation as the most appropriate method for determining the wettability of fine solids isolated from Alberta oil sand [60]. Using film flotation, the mean critical surface tension ($\overline{\gamma_c}$) for rich-grade fine solids (0-66% floating) was ~41.5± 20.8mN/m. Comparing this to sessile drop contact angle suggest that rich-grade fines are heterogeneous and may contain some hydrophobic particles or biwettable fractions [60]. For low-grade fine solids, almost no particle floated on the surface on the solution for the entire range of surface tension tested, which suggested that low-grade fines are very hydrophilic, much more than implied by the 42.4° obtained by sessile drop contact angle method. The higher hydrophilicity of low-grade fines is in agreement with the correlation to fine content observed in Nikakhtari et al. [35]. The contact angle for rich-grade and low coarse solids were obtained by Washburn capillary rise method and were 74.5° and 53.0° respectively. For each sample grade, a comparison of the wettability of fine and coarse solids shows that the fine solids are more hydrophilic than the coarse solids as predicted. The wettability of the fine solids may be attributed to the higher inorganic carbon content (carbonates) and polar residual toluene insoluble organic carbon [71, 72].

3.6.4 Drying curves and residual solvent for reconstituted gangue containing 0%, 10%, and 20% fine solids content

To further support our hypothesis and eliminate any bias in comparison arising from the differences between the two grades of gangue, we performed more experiments on rich-grade samples. Using fine solids and coarse solids obtained only from rich-grade ore, we prepared rich-

grade samples containing 0%, 10%, and 20% fine solids and performed drying experiment under controlled condition for 12% cyclohexane only and then 12% cyclohexane plus 3.7 %* water.
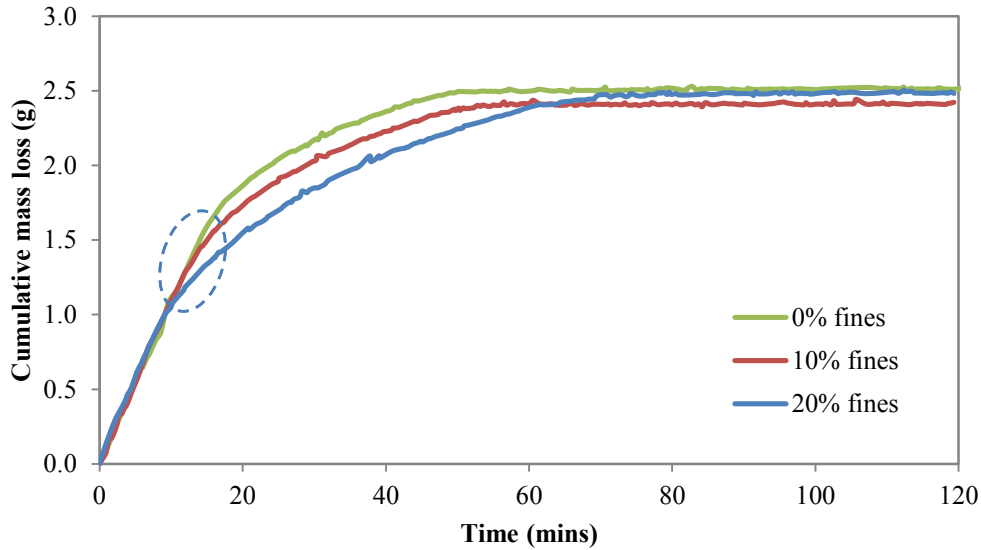
Figure 28: Drying curve for Rich-grade re-gangue containing 12% CH

Table 9: Results for drying of Rich-grade re-gangue containing 12% CH

Fine solids content (wt %)	Duration of stage 1 evaporation of cyclohexane (mins)	Residual cyclohexane (ppm)
0	18.5 ± 1.4	1.1 ± 0.2
10	16.8 ± 1.8	4.1 ± 0.3
20	13.3 ± 2.3	14.7 ± 1.6

3.7W + 12CH
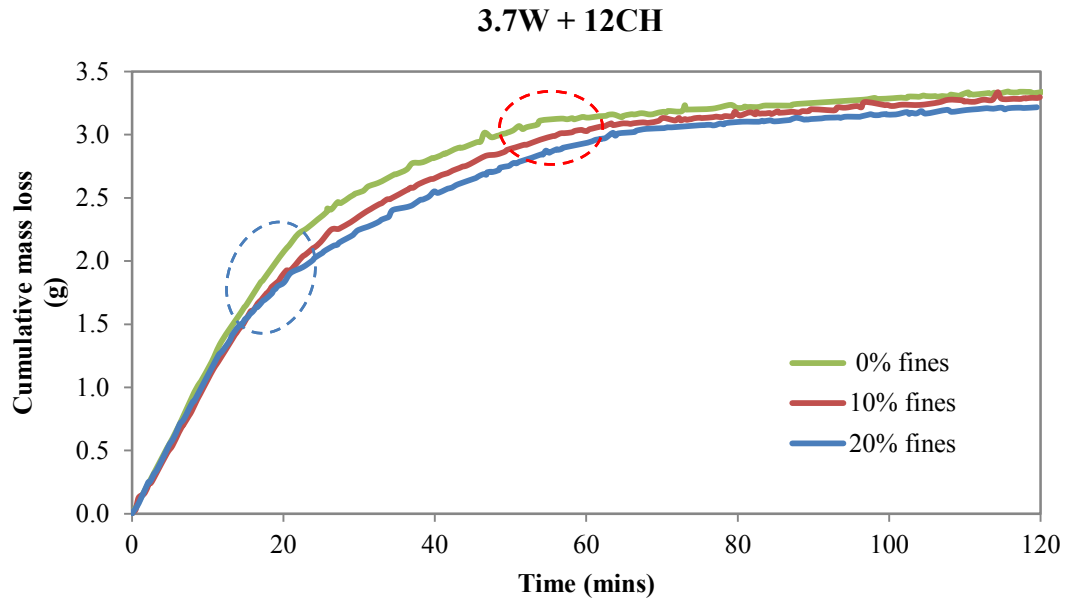
Figure 29: Drying curve for Rich-grade re-gangue containing 12% CH and 3.7%* W

Table 10: Results for drying of Rich-grade re-gangue containing 12% CH and 3.7%* W

Fine solids content (wt %)	Duration of stage 1 cyclohexane evaporation (min)	Transition time (min)	Residual cyclohexane (ppm)
0	23.6 ± 2.1	52.2 ± 0.5	24.6 ± 4.9
10	19.0 ± 1.0	58.6 ± 1.3	27.0 ± 2.3
20	18.4 ± 2.1	65.1 ± 2.1	32.1 ± 3.4
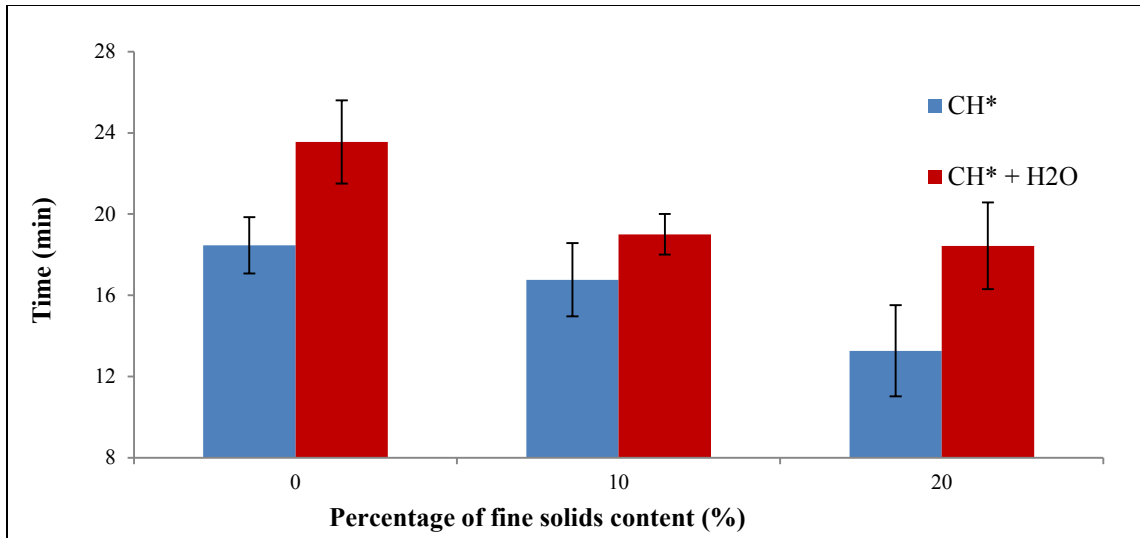
Figure 30: Duration of Stage 1 solvent evaporation in Rich-grade re-gangue
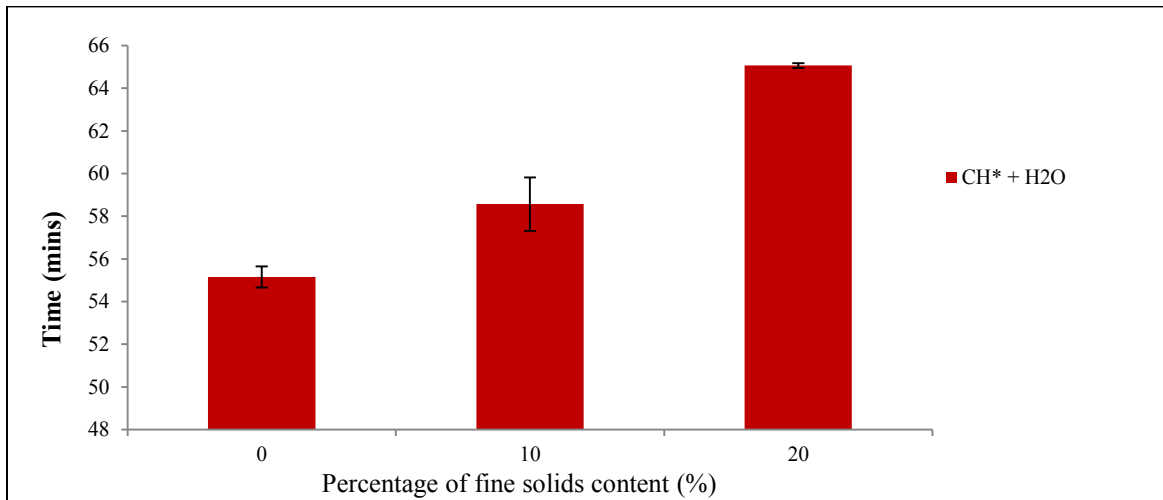
Figure 31: Transition time vs. fine solids content for Rich-grade re-gangue
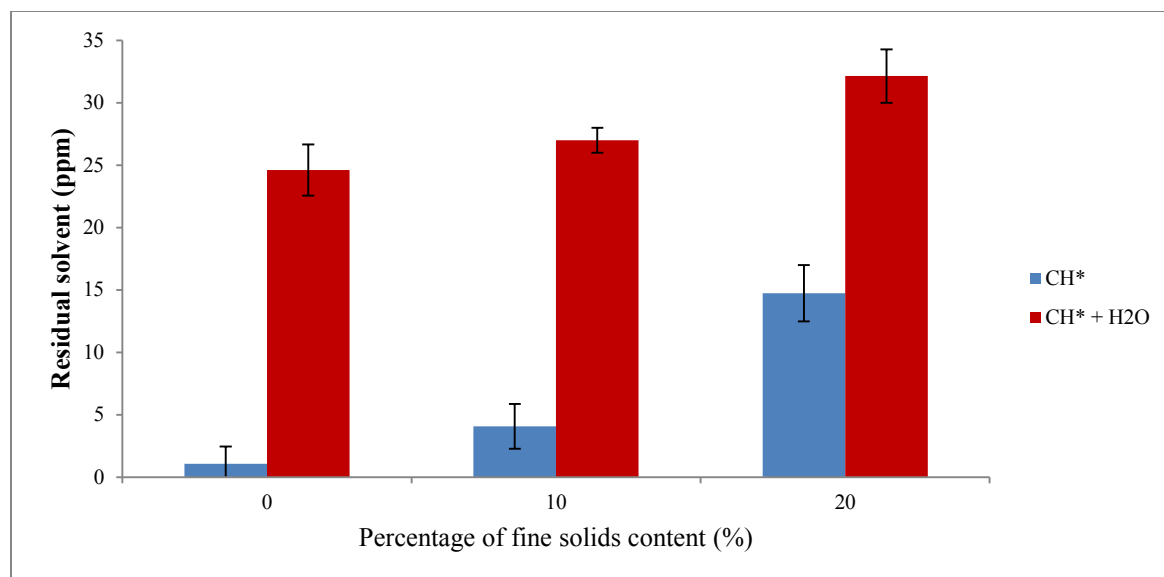
Figure 32: Residual solvent content for Rich-grade re-gangue

In Figures 28 and 29 above, the blue circled region corresponds to the end of stage 1 cyclohexane evaporation (transition to the slower stage 2 evaporation) while red corresponds to the transition from cyclohexane-dominated to water-dominated drying. Figure 30 to 32 are pictorial representations of the analytical result for the drying of rich-grade re-gangue with 0%,10%, and 20% fine solids. The blue bars represent sample containing only 12% CH while red bar represents samples with 12%CH and 3.7 %*W.

It is apparent from Table 9 and Figure 30 that the duration of the fast stage 1 evaporation of cyclohexane decreases as the fine solid content increases. Also, there was an increase in the residual cyclohexane content of the samples as the fine solids content increased; this is indicated by the increase in residual cyclohexane concentration from 1ppm to 14 ppm when the fine solids content increased from 0% to 20%.

Just like samples containing only cyclohexane, samples containing both water and cyclohexane showed a similar trend of a decrease in the duration of stage 1 cyclohexane evaporation as the

fine solids content of the samples increased. Consequently, for these samples, the transition from the cyclohexane-dominated to water-dominated drying occurred at an increasing later stage, as the fine solid content increases. As explained before, this is intuitive because the shorter the duration of stage 1 evaporation, the greater the amount of solvent that has to be evaporated through the slower stage 2 evaporation. Although the residual cyclohexane content for sample containing water showed an increase with increasing fine content, the difference was not as significant as in the samples containing only cyclohexane. Siddhant et al. showed some correlation between the transition time and residual cyclohexane content during the drying of reconstituted rich-grade gangue containing bitumen [31]. They found that so long as the transition time was reached before 80mins of drying, which was the case for the lowest bitumen content analyzed (0.5% Bit.C samples), the residual cyclohexane content did not exceed 200ppm. This observation appears to be the case in our drying experiment containing water. That is because the transition time occurred early (52-65 mins) before the end of the drying experiment (120mins), most of the cyclohexane was removed, and the residual content approached a similar level. The role of water in solvent removal has not been investigated, but it is possible that water blocks the path of some evaporating cyclohexane. In sample containing cyclohexane only, residual cyclohexane is probably trapped in micropores that are unoccupied in the absence of water. Ruiz et al. suggest that in the gas phase, aliphatic VOCs like cyclohexane exhibit a weak van der Waal's adhesion in the soil [74]. However, they reported decreased retention of VOC gas molecules at low concentration in the presence of water or humidity [74]. Ong et al. also found that vapor diffusion of organic contaminant in soil was restricted by moisture [75] Thus, based on our result, it is possible that although less cyclohexane was trapped in the pore in the presence of water, some may be trapped within islands of water .

Another observation made visually from the drying curves and by analysis is that the initial evaporation flux during drying does not change as the fines content change. This observation is consistent with previous works in the literature involving changes in particle size distribution or wettability [52, 67]. No substantial explanation was provided for this observation. From our observation, we see that the presence of fine solids does not affect the rate of the initial stage1 evaporation; rather, it affects the duration of this constant rate period.
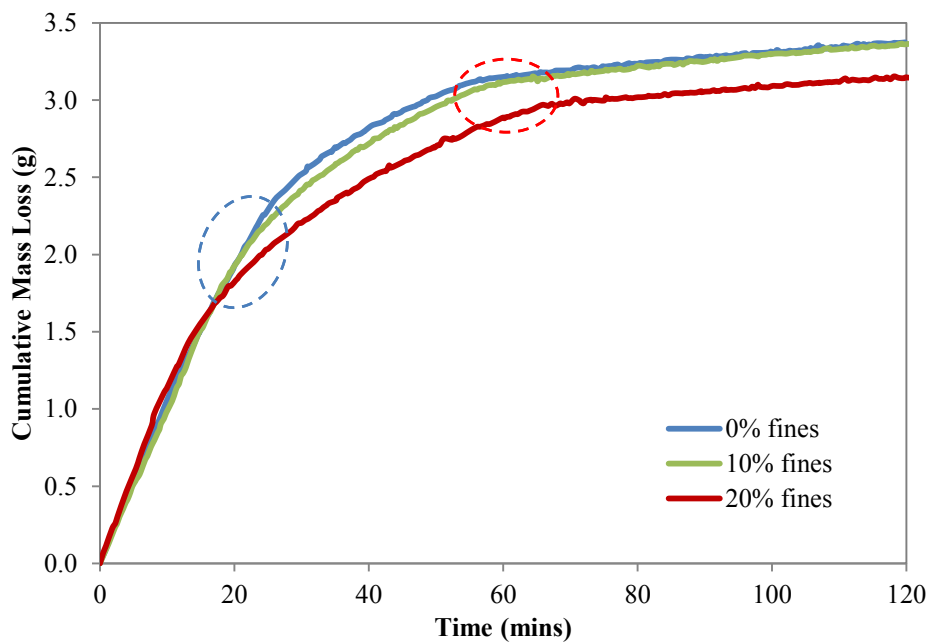
Figure 33: Drying curve for Low-grade re-gangue containing 12% CH and 3.7 %* W

Table 11: Results for drying of Low-grade re-gangue containing 12% CH and 3.7 %* W

Fine solids content (wt %)	Duration of stage 1 cyclohexane evaporation (min)	Transition time (min)	Residual cyclohexane (ppm)
0	22.7	52	19
10	21.2	57	22
20	15.5	65	28

A single experiment was performed for Low-grade re-gangues containing 12 % CH and 3.7 %* W. As shown in Figure 33, a similar trend of the effect of fine solids on the duration of stage 1 evaporation as with rich-grade were made for low-grade re-gangue samples containing 0%, 10% and 20% fine solids for the evaporation of cyclohexane in the presence of 3.7 %* water. Table 11 reveals that the duration of stage 1 evaporation decrease while both the transition time and residual cyclohexane increased as fine solids content is increased for low-grade samples.

On the basis of the literature, results, and discussion presented so far, we can conclude that fine solids decrease the rate of solvent removal during the drying of reconstituted gangue.

The discussion presented in this paper is a simple but sound analysis for the influence of fine solids on solvent recovery. However, to be complete, it is worth mentioning that the drying process is a complex process. As Prat (2007) stated, predictions of drying rate of porous media is a challenging task, complicated by the dependence of drying rates on pore space geometry and local wettability condition [38]. Other intricate changes (in addition to the changes in pore size and wettability) occur in a sample as fine solids content increases. Some of these changes include

a decrease in gravity effect, an increase in viscous dissipation, and a change in pore corner roundness, all of which contribute to the extent of the film region.

Gravity effect decreases with decreasing size of the pores and so favors an increased duration of capillary flow for smaller size particles [45]. Viscous resistance introduces additional flow constraint in finely textured media [49]. However, this effect mainly plays a role in the gas phase than liquid phase [41]. In the gas phase, small pores created by fine particles lead to a more tortuous path for vapor diffusion thereby slowing down vapor diffusion. Also, viscous effects are significant in a network of small pores with narrow size distribution [42, 76], which is not the case for our samples studied. The addition of fine solids to coarse solid as performed in our latter experiments widens the particle size distribution, rather than narrow it. A wider particle size distribution should favour an increase in the duration of stage 1 evaporation [47].

Corner roundedness describes the pore wall microstructure of a porous media, which has a significant effect on the extent of film region [46]. Yiotis et al. showed that flow resistance in porous media is larger for higher values of corner roundedness (*p*), leading to shorter liquid films [46]. Corner roundedness is related to the roughness of the pore wall, but it is independent of pore size [45]. Porous media such as oil sands gangue with rough walls typically have p values that approach zero [45] and at such do not show a dependence on slight changes in corner roundedness. Other factors such as the thickness of the external mass transfer layer (described by the Sherwood number) also affect drying rate. However, the Sherwood number was kept constant throughout the experiments by fixing the bed height.

Although all these factors are not believed to contribute significantly to our case, they could not be investigated during the time frame of this research. Nevertheless, the observation and

conclusion from our experiments on the role of fine solids in decreasing the rate of solvent recovery and thus increasing solvent retention are accurate.

4 Conclusion

Non-aqueous extraction process using cyclohexane as a solvent was applied to extract bitumen from two different Alberta oil sands ore. The composition of the ores was determined by Dean-Stark extraction and fine solids analysis. Rich-grade ore had 13.5 % Bitumen, 3.0% water, and 11% fine solids while low-grade ore had 6.8% bitumen, 9.5% water and ~20% fine solids. Bitumen recovery was calculated using the carbon content obtained from CHNS analysis of the oil sand ore, soxhlet gangue, extracted bitumen, and gangue. The bitumen recovery was over 94% for rich-grade gangue and about 63% for low-grade gangue. Dean-Stark extraction of the gangues and Karl Fisher titration of the product bitumen revealed that almost all the water present in the ores were retained in the gangue. Centrifugation of bitumen product also showed that less than 1% of the total solids in the ore were transferred to the bitumen for both rich-grade and low-grade samples. Only fine solids migrated into the bitumen product, and the amount of solids migrating was fewer in low-grade ore than in rich-grade ore. The wettability of the fine solids and the water content of the gangue had a significant effect on the migration of fine solids [35]. Connate water played a crucial role in binding up fine solids and retaining them in the gangue [35].

Drying experiments were performed for the low-grade gangues and drying curve obtained by plotting cumulative mass loss vs. time. Bitumen migration resulted in a bitumen-enriched top layer and a bitumen-deficient bottom layer during the drying of low-grade gangue. This observation was consistent with observations in previous work of bitumen migration during the drying of rich-grade gangue [28, 31]. Lumps formed during the drying of low-grade gangue, which was attributed to fine solids aggregation due to the high water content of the gangue. Compositional analysis of low-grade gangues revealed that the composition of the gangue varied with each batch of extraction, thus presenting a challenge with studying the interaction of gangue components and their effects on solvent recovery from the gangue.

A protocol was successfully developed for preparing synthetic samples (reconstituted gangue) that mimic the drying behavior of the extracted gangue. The gangues were prepared using similar composition of the extracted gangue and drying experiments were carried out under similarly controlled condition. Both bitumen migration and lump formation were observed for the reconstituted gangue. Analysis of the drying curve (initial flux, transition time and final flux), bitumen enrichment ratio, and bitumen migration fraction confirmed the consistency in drying behavior between the extracted and reconstituted gangue. The reconstituted gangues were important as controlled sample whose composition could be systemically modified, to permit the study of the effect of the gangue variables on solvent recovery from the gangue.

The effect of bitumen on solvent recovery had already been extensively studied in previous work [31]. Bitumen was found to decrease solvent recovery and increase retention in the reconstituted gangue. Consequently, bitumen was excluded from our experiments so as to study the effect of fine solids on the recovery of solvent effectively. Reconstituted gangue of rich-grade and low-grade reconstituted gangues of similar compositions were prepared. Drying experiments were

performed at ambient temperature and pressure, constant bed height and porosity. For samples containing only cyclohexane (12 %), a longer time was required to remove the cyclohexane from the low-grade (high fine) sample than rich-grade (low fines). The low-grade samples had shorter duration of stage 1 evaporation (high rate period of drying in which liquid films sustain capillary connectivity to the surface of the drying media). The residual solvent content was also considerably higher for the low-grade samples than for rich-grade sample. Similarly, for samples contain both 12% cyclohexane and 3.7%* water, the transition time interval (the region where the drying kinetics switches from solvent-dominated to water-dominated drying) occurred at a later time for the low-grade sample, implying a slower solvent removal rate. For these samples, the residual solvent content was only slightly high for low-grade sample compared to rich-grade samples.

Fine solids have a particle size less than 44 µm, and fine solids from non-aqueous extraction are known to be hydrophilic [35, 60]. Thus, both particle (pore) size distribution and wettability of the drying sample changes as the fine solids are added. The influences of these changes were examined by analyzing previous works. Literature suggested that the increase in capillary pressure and the number of fine pores (preferential drying sites at the surface) which arise from smaller particle size increases the duration of the fast rate stage 1 evaporation [45, 49, 67]. On the other hand, a decrease in wettability of the pore walls results in shorter liquid films and a decrease in the duration of stage 1 evaporation [52, 53]. Preliminary results suggested that the effect of wettability change outweighed the effect of a change in particle size distribution. Particle size distribution of the solids was analyzed using a laser particle size analyzer. The wettability of the solids was analyzed using three different methods. Results confirmed that fine solids were more hydrophilic than the coarse solids in both rich-grade and low-grade ore. Low-

grade solids were more hydrophilic than the corresponding rich-grade solids. No significant difference was observed between the particle size distribution of rich-grade and low-grade fine solids. However, the low-grade gangue had a large fraction of smaller sized coarse solids compared to rich-grade.

More controlled experiments were performed to eliminate the influence of the differences in the PSD and wettability between the two grades of samples, thereby permitting appropriate analysis. Reconstituted gangues of different composition of fine solids (0%, 10%, 20%) were prepared by mixing fine and coarse solids obtained from rich-grade only. Two set of these samples, one containing only 12% cyclohexane and the other containing both 12% cyclohexane and 3.7%* water were analyzed. Results from both samples showed the same trend. As the fine solid content of the gangue increase from 0% to 20%, the duration of stage 1 evaporation decreased. Also, for samples with both water and cyclohexane, the transition time decreased with increasing fine solids content. In addition, for samples containing only cyclohexane, there was a distinct difference in the residual solvent content, which increased with increasing fine solids content. Although samples containing water and cyclohexane showed a slight increase in residual solvent content with increasing fines content, the difference was not as larger as those of samples containing only cyclohexane. In the absence of water, residual cyclohexane vapors remain trapped in small pores. When water is present, some pores may be occupied by water while cyclohexane is trapped within water clusters.

The conclusion from these experiments is that fine solids reduce the rate of solvent recovery and lead to increased retention of solvent in the gangue. Another interesting observation was that the initial flux was the same for all samples in a given set of experiment. For example, all three samples (0%, 10%, and 20%) containing water and cyclohexane had similar initial dry flux.

Sample containing only cyclohexane had a similar trend of a constant value of initial flux. More interestingly, even the rich-grade (10%) and low-grade (20%) samples of similar liquid composition in the preliminary experiments had comparatively similar initial drying flux. This observation implied that increasing the fine solids content does not affect the rate of the stage 1 evaporation; rather, it affects the duration of this stage.

5 Future Work

The research study was successful and provided insight into the role of fine solids in non-aqueous extraction. The suggestions presented below are in view of improving future experiments relating to fines solids and the non-aqueous extraction process in general.

When performing non-aqueous extraction of low-grade oil sand gangue, the ore should be milled properly to break up the clumps that form due to high water and fines content. While using the extraction procedure outlined in the paper, the bulk of the bitumen recovery occurred in the first stage of extraction in which mechanical vibration was not applied. For the stage, bitumen present within existing lumps may not be exposed to sufficient solvent during the extraction, thereby contributing to a lower bitumen recovery.

Migration of fine solids into the product bitumen reduces the quality of the product. Therefore, it is advantageous to reduce fine solids migration as much as possible or to remove migrated fine solids. Centrifugation is possible on an industrial scale but is likely to be expensive. Polymers have been used in water management and tailings treatment to facilitate the flocculation and

settling of fine solids in tailings [77]. The polymers work by acting as a bridge between the fine solids. Research should be conducted to explore the use of polymeric flocculants to reduce the fine solid content of bitumen product. Such a polymer should be able to settle out of solution or be separated out by sieving.

Although viscous effect and corner roundness were not expected to contribute significantly to the extent of liquid film in our experiments, it would be insightful to investigate the change in these factors as fine solids content change and also to access their actual contribution to the drying process

Connate water was found to be useful in binding and retaining fine solid in the gangue [35]. However, its role in solvent recovery is not well understood. Water may block the path of the evaporating solvent or trap it in the gangue. More work is required to clarify its role in the removal of solvent especially in the latter stages of the drying process.

Any upscale of the non-aqueous extraction procedure would require a comprehensive predictive solvent recovery model. A solvent recovery model should be developed that incorporates the effect of the different components of the gangue on solvent recovery. Such a model would provide important data in support for the upscale of the non-aqueous extraction process.

Bibliography

[1]   Masliyah, J.; Czarnecki, J.; Xu, Z. *Handbook on Theory and Practice of Bitumen Recovery from Athabasca Oil Sands*; Kingsley Knowledge Publishing: Canada, 2011.

[2]   Government of Alberta. Alberta's Oil Sands: The Facts. January, 2014

[3]   Gray, M. R. *Upgrading Oilsands Bitumen and heavy oil*; University of Alberta Press: Canada, 2015.

[4]   Pal, K.; Branco, Lucas da Paz Nogueira; Heintz, A.; Choi, P.; Liu, Q.; Seidl, P. R.; Gray, M. R. Performance of Solvent Mixtures for Non-aqueous Extraction of Alberta Oil Sands. *Energy & Fuels* **2015**, *29*, 2261-2267.

[5]   Energy Resources Conservation Board. ST98-2012: *Alberta's Energy Reserves 2011 and Supply/Demand Outlook 2012−2021*; Energy Resources Conservation Board: Edmonton, Alberta, Canada, 2012.

[6]   Regional Aquatic Monitoring Program. http://www.rampalberta.org/resources/development/history/insitu.aspx (Accessed Jul 9, 2016).

[7]   Das, S. K.; Butler, R. M. Mechanism of the vapor extraction process for heavy oil and bitumen. *Journal of Petroleum Science and Engineering* **1998**, *21*, 43-59.

[8]   Hooshiar, A.; Uhlik, P.; Liu, Q.; Etsell, T. H.; Ivey, D. G. Clay minerals in nonaqueous extraction of bitumen from Alberta oil sands: Part 1. Nonaqueous extraction procedure. *Fuel Processing Technology* **2012**, *94*, 80-85.

[9] Noorjahan, A.; Tan, X.; Liu, Q.; Gray, M. R.; Choi, P. Study of Cyclohexane diffusion in Athabasca Asphaltenes. *Energy & Fuels*, **2014**, *28*(2), 1004–1011.

[10] Alberta Energy Regulator. ST98-2015: *Alberta's Energy Reserves 2014 and Supply/Demand Outlook 2015-2024*; Alberta Energy Regulator: Calgary, Alberta, Canada. 2014

[11] Dyer, S; Huot, M.; Mining vs In situ: Fact Sheet. Pembina Institute: Calgary, Alberta, Canada. 2010

[12] AMEC Earth and Environment. *Current and Future Water Use in Alberta*. Alberta Environment, Edmonton, Alberta, Canada. 2007

[13] Sauchyn, D. J.; St-Jacques, J.-M.; Luckman, B. H. Long-term reliability of the Athabasca river (Alberta, Canada) as the water source for oil sands mining. *Proceedings of the National Academy of Sciences*, **2015**, *112*(41), 12621–12626.

[14] Government of Alberta. Oil Sands Tailing. September 2013

[15] Schindler, D. W. Unravelling the complexity of pollution by the oil sands industry. *Proceedings of the National Academy of Sciences* **2014***, 111*, 3209-3210.

[16] Kelly, E. N.; Short, J. W.; Schindler, D. W.; Hodson, P. V.; Ma, M.; Kwan, A. K.; Fortin, B. L. Oil sands development contributes polycyclic aromatic compounds to the Athabasca river and its tributaries. *Proceedings of the National Academy of Sciences*, 2009, *106*(52), 22346–22351.

[17] Frank, R. A.; Roy, J. W.; Bickerton, G.; Rowland, S. J.; Headley, J. V.; Scarlett, A. G.; West, C. E.; Peru, K. M.; Parrott, J. L.; Conly, F. M.; Hewitt, L. M. Profiling oil sands mixtures from industrial developments and natural groundwaters for source identification. *Environmental science & technology* **2014**, *48*, 2660.

[18] Small, C. C.; Cho, S.; Hashisho, Z.; Ulrich, A. C. Emissions from oil sands tailings ponds: Review of tailings pond parameters and emission estimates. *Journal of Petroleum Science and Engineering* **2015**, *127*, 490-501.

[19] Coulson, G. R. Process for separating oil from bituminous sands, shales, etc. US 2825677 A, March 04, 1958.

[20] Meadus, F. W.; Chevrier, P. J.; Sparks, B. D. Solvent extraction of Athabasca oil-sand in a rotating mill Part 1. Dissolution of bitumen. *Fuel Processing Technology* **1982**, *6*, 277-287.

[21] Painter, P.; Williams, P.; Mannebach, E. Recovery of Bitumen from oil or tar sands using ionic liquids. *Energy & Fuels*, 2010, *24*(2), 1094-1098.

[22] Painter P.; Williams, P.; & Lupinsky, A. Recovery of Bitumen from Utah tar sands using ionic liquids. *Energy & Fuels*, 2010, *24*(9), 5081–5088.

[23] Wang, T.; Zhang, C.; Zhao, R.; Zhu, C.; Yang, C.; Liu, C. Solvent Extraction of Bitumen from Oil Sands. *Energy & Fuels* **2014**, *28*, 2304.

[24] Leung, H.; Phillips, C. R. Solvent extraction of mined Athabasca oil sands. *Industrial & Engineering Chemistry Fundamentals* **1985**, *24*, 373-379.

[25] Wu, J.; Dabros, T. Process for Solvent Extraction of Bitumen from Oil Sand. *Energy & Fuels* **2012***, 26*, 1002-1008.

[26] Nikakhtari, H.; Vagi, L.; Choi, P.; Liu, Q.; Gray, M. R. Solvent screening for non-aqueous extraction of Alberta oil sands. *The Canadian Journal of Chemical Engineering* **2013***, 91*, 1153-1160.

[27] Hansen C. M. Hansen Solubility Parameters: A User's Handbook; CRC Press (Taylor & Francis Group): Boca Raton, FL, 1999.

[28] Renaud, R. *A study on the effect of temperature and pressure on the removal of cyclohexane from non-aqueous extraction gangue.* MSc. Dissertation, University of Alberta, 2014.

[29] Li X.; He, L.; Wu, G.; Sun, W.; Li, H.; Sui, H. Operational parameters, evaluation methods, and fundamental mechanisms: Aspects of nonaqueous extraction of bitumen from oil sands. *Energy & Fuels,* 2012, *26(6), 3563.*

[30] Cormack, D. E.; Kenchington, J. M.; Phillips, C. R.; & Leblanc, P. J. Parameters and mechanisms in the solvent extraction of mined athabasca oil sand. *The Canadian Journal of Chemical Engineering*, 1977, *55*(5), 572-580.

[31] Panda S., *Role of Residual Bitumen on the Solvent Removal from Alberta Oil Sands Gangue*. MSc. Dissertation, University of Alberta, 2015.

[32] Yu, K.; Wang, Z.; Jin, Y.; Sun, Z.; Liu, Y.; Yang, J.; Cai, Y. Single- and multi-stage counter-current solvent Extractions of Bitumen from Xinjiang oil sand. *Energy & Fuels*, *27*(11), 2013, 6491-6500.

[33] Nikakhtari, H.; Pal, K.; Wolf, S.; Choi, P.; Liu, Q.; Gray, M. R. Solvent removal from cyclohexane-extracted oil sands gangue. *The Canadian Journal of Chemical Engineering* **2016**, *94*, 408-414.

[34] Dang-Vu T.; Jha, R.; Wu, S.-Y.; Tannant, D. D.; Masliyah, J.; Xu, Z. Effect of solid Wettability on Processability of oil sands ores. *Energy & Fuels*, **2009**, *23*(5), 2628-2636.

[35] Nikakhtari, H.; Wolf, S.; Choi, P.; Liu, Q.; Gray, M. R. Migration of fine solids into product Bitumen from solvent extraction of Alberta Oil Sands. *Energy & Fuels*, 2014, *28*(5), 2925-2932.

[36] Ruiz, J.; Bilbao, R.; Murillo, M. B. Adsorption of Different VOC onto Soil Minerals from Gas Phase: Influence of Mineral, Type of VOC, and Air Humidity. *Environmental Science & Technology,* **1998**, *32*, 1079-1084.

[37] Serrano, A.; Gallego, M. Sorption study of 25 volatile organic compounds in several Mediterranean soils using headspace–gas chromatography–mass spectrometry. *Journal of Chromatography,* **2006**, *A1118*, 261-270.

[38] Prat, M. On the influence of pore shape, contact angle and film flows on drying of capillary porous media. *International Journal of Heat and Mass Transfer* **2007**, *50*, 1455-1468.

[39] Yiotis, A. G.; Boudouvis, A. G.; Stubos, A. K.; Tsimpanogiannis, I. N.; Yortsos, Y. C. Effect of liquid films on the isothermal drying of porous media. *Physical review. E, Statistical, nonlinear, and soft matter physics* **2003**, *68*, 037303.

[40] Yiotis, A. G.; Boudouvis, A. G.; Stubos, A. K.; Tsimpanogiannis, I. N.; Yortsos, Y. C. Effect of liquid films on the drying of porous media. *AIChE Journal* **2004***, 50*, 2721-2737.

[41] Yiotis, A. G.; Stubos, A. K.; Boudouvis, A. G.; Yortsos, Y. C. A 2-D pore-network model of the drying of single-component liquids in porous media. *Advances in Water Resources* **2001***, 24*, 439-460.

[42] Prat, M.; Bouleux, F. Drying of capillary porous media with a stabilized front in two dimensions. *Physical review. E, Statistical physics, plasmas, fluids, and related interdisciplinary topics* **1999***, 60*, 5647-5656.

[43] Laurindo, J. B.; Prat, M. Numerical and experimental network study of evaporation in capillary porous media. Drying rates. *Chemical Engineering Science* **1998***, 53*, 2257-2269.

[44] Plourde, F.; Prat, M. Pore network simulations of drying of capillary porous media. Influence of thermal gradients. *International Journal of Heat and Mass Transfer*, 2003, *46*(7), 1293–1307.

[45] Yiotis, A. G.; Salin, D.; Tajer, E. S.; Yortsos, Y. C. Drying in porous media with gravity-stabilized fronts: experimental results. *Physical review. E, Statistical, nonlinear, and soft matter physics* **2012***, 86*, 026310.

[46] Yiotis, A.; Salin, D.; Yortsos, Y. Pore Network Modeling of Drying Processes in Macroporous Materials: Effects of Gravity, Mass Boundary Layer and Pore Microstructure. *Transp Porous Med* **2015***, 110*, 175-196.

[47] Lehmann, P.; Assouline, S.; Or, D. Characteristic lengths affecting evaporative drying of porous media. *Physical review. E, Statistical, nonlinear, and soft matter physics* **2008***, 77*, 056309.

[48] Suzuki, M.; Maeda, S. On the Mechanism of Drying of Granular Beds. *Journal of Chemical Engineering of Japan*, **1968***, 1(1)*, 26-31.

[49] Lehmann, P.; Or, D. Evaporation and capillary coupling across vertical textural contrasts in porous media. *Physical review. E, Statistical, nonlinear, and soft matter physics* **2009***, 80*, 046318.

[50] Abdallah et al. *Fundamentals of Wettability (oilfield review)*. http://www.slb.com/resources/publications/industry_articles/oilfield_review/2007/or2007sum04_wettability.aspx. (accessed July 11, 2016)

[51] Israelachvili, J. N. *Intermolecular and surface forces* , 3rd ed.; United States: Academic Press. 2011

[52] Shokri, N.; Lehmann, P.; Or, D. Characteristics of evaporation from partially wettable porous media. *Water Resources Research* **2009***, 45*, W02415.

[53] Shokri, N.; Or, D. Drying patterns of porous media containing wettability contrasts. *Journal of colloid and interface science* **2013***, 391*, 135-141.

[54] Satorius. Manual of weighing application. http://www.dcu.ie/sites/default/files/mechanical_engineering/pdfs/manuals/DensityDeterminationManual.pdf (accessed July 29, 2016)

[55] Pasternack S.; Clark K. A. *The Components of the Bitumen in Athabasca Bituminous Sand and their Significance in the Hot Water Separation Process. 1951.*

[56]   de Klerk, A.; Gray, M. R.; Zerpa, N. Unconventional oil an d gas:Oilsands. In Future Energy, 2nd ed.; Letcher, T. M., Ed.; Els evier:Amsterdam, Netherlands, 2014; Chapter 5, pp 95−116.

[57]   Mckenzie, N.; Coughlan, K.; Cresswell, H. *Soil Physical Measurement and Interpretation for Land Evaluation. Collingwood, Vic.: CSIRO Pub., 2002.*

[58]   Thermo Scientific Inc. Flash 2000 Series, CHN/CHNS/Oxygen Automatic Elemental Analyzer. CEElantech website.

http://s3.ceelantech.com/docs/AN641_Carbon_Fiber_2000.pdf   (accessed   June   22, 2016)

[59]   http://www.malvern.com/en/products/product-range/mastersizer-range/mastersizer-3000/ (accessed July 10, 2016)

[60]   Wang, C.; Geramian, M.; Liu, Q.; Ivey, D. G.; Etsell, T. H. Comparison of different methods to determine the surface Wettability of fine solids isolated from Alberta Oil sands. *Energy & Fuels*, **2015,** *29*(6), 3556–3565.

[61]   Dang-Vu, T.; Jha, R.; Wu, S.; Tannant, D. D.; Masliyah, J.; Xu, Z. Wettability determination of solids isolated from oil sands. *Colloids and Surfaces A: Physicochemical and Engineering Aspects* **2009***, 337*, 80-90.

[62]   Diao, J.; Fuerstenau, D. W. Characterization of the wettability of solid particles by film flotation 2. Theoretical analysis. *Colloids and Surfaces* **1991***, 60*, 145-160.

[63] Fuerstenau, D. W.; Diao, J.; Williams, M. C. Characterization of the wettability of solid particles by film flotation 1. Experimental investigation. *Colloids and Surfaces*, 1991, *60*, 127–144.

[64] Galet, L.; Patry, S.; Dodds, J. Determination of the wettability of powders by the Washburn capillary rise method with bed preparation by a centrifugal packing technique. *J. Colloid Interface Sci.* **2010***, 346*, 470-475.

[65] Ryan, S. E.; Porth, L. S. *A tutorial on the piecewise regression approach applied to bedload transport data.* Fort Collins, CO: U.S. Dept. of Agriculture, Forest Service, Rocky Mountain Research Station, 2007.

[66] Scherer, G. W. Theory of Drying. *Journal of the American Ceramic Society* **1990***, 73*, 3-14.

[67] Rad, M.; Shokri, N.; Keshmiri, A.; Withers, P. Effects of Grain and Pore Size on Salt Precipitation During Evaporation from Porous Media. *Transp Porous Med* **2015***, 110*, 281-294.

[68] Sghaier, N.; Prat, M. Effect of Efflorescence Formation on Drying Kinetics of Porous Media. *Transport in Porous Media* **2009***, 80*, 441-454.

[69] Al-Futaisi, A.; Patzek, T. W. Impact of wettability alteration on two-phase flow characteristics of sandstones: A quasi-static description. *Water Resources Research* **2003***, 39*, 1042.

[70] Wallach, R.; Margolis, M.; Graber, E. R. The role of contact angle on unstable flow formation during infiltration and drainage in wettable porous media. *Water Resources Research* **2013***, 49*, 6508-6521.

[71] Osacky, M.; Geramian, M.; Ivey, D. G.; Liu, Q.; Etsell, T. H. Mineralogical and chemical composition of petrologic end members of Alberta oil sands. *Fuel* **2013**, *113*, 148-157.

[72] Dongbao F.; Woods, J.R.; Kung, J.; Kingston, D.M.; Kotlyar, L.S.; Sparks, B.D.; Mercier, P.H.J.; McCracken, T.; Ng, S. Residual organic matter associated with Toluene-Extracted oil sands solids and its potential role in Bitumen recovery via Adsorption onto Clay Minerals, *Energy & Fuels*, 2010, 24, 2249–2256.

[73] Hooshiar, A.; Uhlik, P.; Ivey, D. G.; Liu, Q.; Etsell, T. H. Clay minerals in nonaqueous extraction of bitumen from Alberta oil sands. *Fuel Processing Technology* **2012**, *96*, 183-194.

[74] Ruiz J.; Bilbao, R.; Murillo, M.B. Adsorption of different VOC onto soil minerals from gas phase: Influence of mineral, type of VOC, and air humidity, *Environmental Science & Technology*, 1998, 32(8), 1079–1084.

[75] Ong, S. K.; Culver, T. B.; Lion, L. W.; Shoemaker, C. A. Effects of soil moisture and physical-chemical properties of organic pollutants on vapor-phase transport in the vadose zone. *Journal of Contaminant Hydrology* **1992**, *11*, 273-290.

[76] Metzger T.; Tsotsas, E. Viscous stabilization of drying front: Three-dimensional pore network simulations. *Chemical Engineering Research and Design* **2008**, *86*, 739-744.

[77] Lu, Q.; Yan, B.; Xie, L.; Huang, J.; Liu, Y.; Zeng, H. A two-step flocculation process on oil sands tailings treatment using oppositely charged polymer flocculants. *Science of the Total Environment* **2016**, *565*, 369-375.

Appendix

Appendix A1 - Bitumen Recovery Calculation

The recovery of bitumen from non-aqueous extraction was defined as the percentage of the total bitumen initially present in the oil sands ore sample extracted into the solvent phase. Equation gives the formula for calculating bitumen recovery

$$\% \ Recovery = \left\{ 1 - \frac{W_t - W_s}{(W_o - W_s)(W_b - W_t + W_s)} * \left[(W_b - W_o + W_s) - \frac{M_c}{M}(W_b - W_c + W_s) \right] \right\}$$

where

W_t = mass fraction of C in the gangue

W_s = mass fraction of toluene-insoluble C in the oil sands

W_o = mass fraction of C in the oil sands

W_b = mass fraction of C in the bitumen

W_c = mass fraction of C in the centrifuge solids

M = mass of oil sands ore used for extraction

M_c = mass of centrifuge solids

Bitumen recovery for low-grade ore was calculated using the following

W_t (%)	W_s(%)	W_o(%)	W_b(%)	W_c(%)	M(g)	M_c(g)
3.09-3.37	1.04	6.76	83.41	-	150	-

No value was obtained for W_c and M_c because the mass of fines migrating to product was negligible and insufficient to carbon mass fraction by CHNS analysis

For W_t in the range of 3.09-3.37, we obtained a bitumen recovery of 63.2 ± 1.9%.

Appendix A2 - Preparation of Reconstituted Gangue

Addition of bitumen

Starting with X g of Soxhlet gangue, let x be the mass of bitumen associated carbon to be added for a target bitumen carbon content of b % where b ranged from 0-2%. The formula for calculating m is

$$\frac{x}{1.2x + X} = \frac{(a + 0.3)}{100}$$

Note:

➤ Due to loss of bitumen (on the walls of the jars, glass, spatula, among others), an additional 0.3% was added to the target bitumen carbon % (when a is greater than zero) as shown in the above equation, in order to attain the target value in the reconstituted samples.

➤ The factor of 1.2 arises from the mass fraction of carbon in bitumen (~0.834) as given by CHNS analysis and literature [55, 56] i.e. 1.2g of bitumen contains 1g of carbon.

The mass of bitumen thus required is given by $m_b = 1.2x$

0.5X g of cyclohexane is used to dissolve $1.2x$ g of bitumen prior to addition of Soxhlet gangue

Addition of Water

Mass of DSBS, $X_B = X + 1.2x$

Let x_w be the mass of water required to attain $w\%$ of water in the gangue. Then

$$\frac{x_w}{x_w + X_B} = \frac{w}{100}$$

The range for $w\%$ was 0-10% (solvent free mass basis).

Addition of Cyclohexane

Mass of WSBS, $X_{BW} = X_B + x_w$

Let x_c be the mass of cyclohexane required to attain $c\%$ of cyclohexane in the gangue. Then

$$\frac{x_c}{x_c + X_{BW}} = \frac{c}{100}$$

The range for c was 12-14%.

Appendix A3 - Film Flotation

The mean critical surface tension, $\bar{\gamma}_c$ of the fine solids is given by

$$\bar{\gamma}_c = \int \gamma_c f(\gamma_c) d\gamma_c$$

where γ_c is the critical surface tension of the solids and $f(\gamma_c)$ is the frequency distribution function [63].

The standard deviation is given as [63]

$$\sigma_{\gamma_c} = \left[\int (\gamma_c - \bar{\gamma}_c)^2 f(\gamma_c) d\gamma_c \right]^{1/2}$$